R. & M. No. 3148
(20,472)
A.R.C. Technical Report

R. & M. No. 3148

MINISTRY OF AVIATION

AERONAUTICAL RESEARCH COUNCIL
REPORTS AND MEMORANDA

Heat-Transfer and Skin-Friction Measurements at a Mach Number of 2·44 for a Turbulent Boundary Layer on a Flat Surface and in Regions of Separated Flow

By G. E. GADD, Ph.D., W. F. COPE, M.A. and J. L. ATTRIDGE, B.Sc.,
OF THE AERODYNAMICS DIVISION, N.P.L.

LONDON: HER MAJESTY'S STATIONERY OFFICE
1960
PRICE: 14s. 0d. NET

Heat-Transfer and Skin-Friction Measurements at a Mach Number of 2·44 for a Turbulent Boundary Layer on a Flat Surface and in Regions of Separated Flow

By G. E. GADD, Ph.D., W. F. COPE, M.A. and J. L. ATTRIDGE, B.Sc.,
OF THE AERODYNAMICS DIVISION, N.P.L.

*Reports and Memoranda No. 3148**
October, 1958

1. *Introductory Remarks concerning Existing Data for Unseparated Layers.* A considerable body of data exists concerning the skin friction, the heat-transfer characteristics, and the wall temperature for zero heat transfer for turbulent boundary layers in supersonic flow in the absence of separation. Experiments have been made with bodies of revolution (Refs. 5, 9, 11, 12, 14, 21, 23, 31, 35, 40, 48, 61, 64, 66 and 71), flat plates (Refs. 15, 16, 18, 26, 34, 42, 43, 44, 45, 49, 53, 58, 59, 60 and 62), wind-tunnel walls (Refs. 4, 8 and 38), or with other arrangements (Ref. 7). Where the streamwise pressure gradient is zero the results can be approximately related to equivalent conditions on a flat plate. These 'equivalent flat plate' data are of great practical use, since the characteristics of turbulent boundary layers in most engineering applications (as, for example, in the flow over the wings of an aircraft), roughly approximate to those of a boundary layer on a flat plate.

A comparison of the experimental findings for boundary layers at constant pressure suggests the following general conclusions:

(*a*) The recovery factor r, defining the recovery temperature or wall temperature for zero heat transfer, is about 0·88 to 0·89, independent of Mach number, for a Reynolds number R_θ, based on momentum thickness, of the order of 10^4 (with a flat plate, the corresponding Reynolds number based on distance from the leading edge is in the range 10^6 to 10^7). With increasing Reynolds number r decreases very slowly.

(*b*) For heat-transfer rates that are not too large (and possibly generally), the ratio of the average Stanton number $\overline{St}$ to the average skin friction coefficient C_F, or of the local Stanton number St to the local skin-friction coefficient C_f, is approximately equal to 0·6 for Reynolds numbers R_θ of about 10^4. It is possible that this ratio also decreases slowly with increasing Reynolds number.

(*c*) The ratio of the average or local skin-friction coefficient or Stanton number to the corresponding quantity in incompressible flow at a related value of R_θ is as shown in Fig. 1, for small rates of heat transfer to the wall. The appropriate incompressible value of R_θ, $R_{\theta i}$, is given by

$$\frac{R_\theta}{R_{\theta i}} = \frac{C_f}{C_{fi}}, \frac{C_F}{C_{Fi}}, \frac{St}{St_i}, \text{ or } \frac{\overline{St}}{\overline{St}_i}. \tag{1}$$

* Published with the permission of the Director, National Physical Laboratory.

This means that for a flat plate, the Reynolds number R_{xe} based on the distance from the effective leading edge of the turbulent boundary layer is the same in the compressible case as in the incompressible case with which it is compared. For the purposes of the present paper it is assumed for simplicity that

$$C_{fi} = 0\cdot0592 R_{xe}^{-1/5} = 0\cdot0259 R_{\theta i}^{-1/4} \tag{2}$$

$$C_{Fi} = 0\cdot0740 R_{xe}^{-1/5} = 0\cdot0324 R_{\theta i}^{-1/4} \tag{3}$$

$$St_i = 0\cdot0355 R_{xe}^{-1/5} = 0\cdot0155 R_{\theta i}^{-1/4} \tag{4}$$

$$\overline{St}_i = 0\cdot0444 R_{xe}^{-1/5} = 0\cdot0194 R_{\theta i}^{-1/4}\,. \tag{5}$$

These relations (*cf*. Ref. 27) are probably accurate to within 5 per cent, at any rate, over the Reynolds-number range for which most of the high-speed data have been obtained, *viz*., $1\cdot5 \times 10^6 < R_{xe} < 10^7$.

Several semi-empirical theories, for example, Refs. 19, 20, 22, 25, 41, 53, 69 and 70, predict curves similar to Fig. 1. However, this curve has actually been derived from a comparison of the available experimental data, most of which concern skin friction. Other reviewers of these data (Refs. 32, 36, 40, 41, 46, 55 and 57) have in the main produced mean curves a little lower than the curve of Fig. 1. Most weight is generally given to Coles's results (Refs. 15 and 16), obtained by means of careful direct-force measurements with a floating element. The data as Coles presents them have been rather elaborately processed, but if reference is made to the original measurements given in Tables 3 and 4 of Ref. 15, it will be found, on application of equations (1) and (2), that all the data lie close to the curve of Fig. 1. Other floating-element measurements of Korkegi[34], when similarly analysed, lie close to this curve. The results of Chapman and Kester[11, 12], obtained from net drag measurements on the parallel part of a cone-cylinder body, lie a little below the curve. This may possibly be due to uncertainties inherent in the experimental method used. All methods are indeed subject to some uncertainties. With the floating-element technique doubts may perhaps arise concerning the effects of the gaps. Application of the momentum equation, which sometimes yields data lying above the curve of Fig. 1, is suspect because of the customary neglect of turbulent normal stresses. The errors arising from this may possibly be considerable at supersonic speeds even when there is zero pressure gradient, as Chapman and Kester[12], citing Ross's analysis[52], have pointed out. With Stanton or half-pitot tubes, or with Preston tubes (circular pitot tubes resting on the surface[50]), compressibility effects may perhaps render inapplicable calibration data obtained in incompressible flow. Thus the precise measurement of skin friction is not easy. Heat-transfer measurements also are just as liable to error. Some methods depend on measuring the rate at which the wall is heated or cooled due to a difference between its initial temperature and the recovery temperature (the wall temperature for zero heat transfer). The extensive measurements of Brevoort and Rashis, for example, summarized in Ref. 7, are of this type. Their results lie considerably above the curve of Fig. 1. In their experiments the variation of wall temperature during the run was not small compared with the difference between the wall temperature and the recovery temperature. For such conditions the instantaneous rates of heat transfer are possibly not the same as they would be if the temperatures were steady. On the other hand, with steady-state measurements, where the surface temperature of the body is maintained constant, and the rate of heating or cooling is measured, it is often difficult to obviate heat leakages. Besides all this, a fundamental source of possible error underlying all work on the characteristics of 'the turbulent boundary layer', is the tacit assumption that the boundary layer studied is uniquely determined by Reynolds number and Mach number. This will not always be true. The existence of pressure gradients upstream of the test section, the use of devices provoking artificial transition, departures from strictly two-dimensional conditions, all such factors must have some influence on the boundary layer. Hence some scatter on the experimental data is to be expected, but this, however, does not greatly matter for practical engineering applications.

2. *Introduction to the Present Experiments.* In the present experiments the test boundary layer was that formed on a flat wind-tunnel liner, over the downstream part of which, where the measurements were made, the Mach number was approximately 2·44 (*see* Fig. 2). Measurements were made of the local heat transfer at two stations by a steady-state technique. The only other published measurements of this type are those of Bradfield and DeCoursin[5, 21], Pappas[49], Shoulberg[58] and Slack[60], so there is a need for further data. Skin-friction measurements were also attempted by means, firstly, of Stanton tubes and secondly, by boundary-layer traverses to determine the momentum thickness.

The results for the heat-transfer characteristics are in broad agreement with the general findings described at the beginning of this Section. The skin-friction results obtained from boundary-layer traverses are of the same order as, though about 10 per cent higher than, the accepted values. The Stanton-tube results converted to local skin-friction coefficients by means of incompressible calibration data are somewhat higher again, about 25 per cent above the accepted values, but this may be due to neglected effects of compressibility. Some of the apparent anomalies in the skin-friction results may be due to the fact that the test boundary layer does not develop under constant pressure right from the start. Be that as it may, it is felt that the results give a useful corroboration of previous findings as regards heat transfer, and that they also show that the techniques used in the present experiments give results which are quite good for heat transfer and at least of the right order for skin friction.

Qualitative results were all that was sought in the second part of the experiment concerning heat transfer and skin friction in regions of separated flow. In contrast with the flat-plate boundary layer, this is a problem that has not been much studied experimentally. In order to produce separated flow in our experiments a slab could be attached at various positions to the surface of the flat liner as in Figs. 2 and 3, forming a forward-facing step, upstream of which separation occurred, and a rearward-facing step, downstream of which the flow reattached. Surface-tube measurements of local skin friction were made through both these regions, and should be less subject to compressibility errors than the readings made in the attached boundary layer. The local heat transfer was also measured, and boundary-layer traverses made. The heat-transfer characteristics of separated flows are of particular interest, since it has been suggested that one way of reducing the heat transfer to very fast-moving aircraft would be to cause the flow to separate from the surface. However, the present experiment shows that such a method of attempting to reduce heat transfer would have to be used with caution, since unexpectedly high rates of heat transfer were encountered just upstream of the forward-facing step, and the heat transfer was also found to be high where the boundary layer reattaches downstream.

3. *Description of the Apparatus.* The experiments were done in the 13 in. × 11 in. continuous compressor-driven tunnel of the National Physical Laboratory. For the present tests, however, the working-section height was reduced to a maximum of 11·4 in. so that the surface of the flat liner, where the boundary-layer measurements were made, was higher than the bottom of the side-wall

windows, and hence was visible for schlieren pictures. In a short expanding section just downstream of the liners it was found necessary to insert a bridge-piece spanning the tunnel as shown in Fig. 2. Without this bridge the flow separated from the flat liner close to the rear measurement station, presumably because of a strong breakdown shock in the expanding section. The separation was more severe when the flat liner was heated. The bridge acted as a second throat and probably replaced the breakdown shock by a system of oblique shocks having a less severe effect on the tunnel boundary layers, so eliminating the separation from the rear of the test liner.

For part of the experiments separation was deliberately provoked as in Fig. 3. The slab used to do this spanned the tunnel completely and was $\frac{15}{16}$ in. high and $12\frac{1}{2}$ in. long. It could be attached to the liner at a number of positions $\frac{1}{2}$ in. apart between the extreme positions indicated in Fig. 2. Since the distance of the separation point, for example, upstream of the step did not change appreciably for small movements of the slab, moving the slab by $\frac{1}{2}$ in. at a time and measuring at fixed stations was equivalent to making a number of measurements at $\frac{1}{2}$ in. intervals in a fixed separated region.

The tunnel window was not large enough to cover the whole field of flow shown in Fig. 3, so that this Figure had to be made up from three separate photographs taken with three different positions of the slab. For this reason, stray weak compression waves associated with small imperfections in the tunnel flow do not match up in the composite picture. However, the main features of the separated flow, such as the compression band from the forward separation point, do match up almost exactly, and this confirms that movements of the slab did not appreciably affect the size of the separated regions.

Underneath the liner were a number of electric fire bars connected in parallel as shown in Fig. 2. These bars would each dissipate 1 kilowatt if 240 volts were applied to them, but the voltage used in the experiment could be varied in small steps between about 20 volts and 170 volts. Thus the average surface temperature of the flat liner could be varied. Typically in heat-transfer tests it was made to be about 65 deg C, with a stagnation temperature of about 40 deg C and a corresponding recovery temperature of about 18 deg C. The surface temperature varied with distance along the liner, because the heat was applied at a number of discrete sources, and the temperature was almost certainly lower near the sides of the tunnel than in the middle of the liner because of the tunnel side walls and also because the fire bars were shorter than the tunnel span. However, the liner was made of an aluminium alloy, a fairly good thermal conductor, and this kept the temperature variation within tolerable limits. Thus when the liner was heated the difference between the lowest measured temperature on the centre-line of the liner and the highest was typically about 16 deg C, and the temperature gradients were quite small close to the measurement stations.

In the liner itself there were three static-pressure tappings and three thermo-couples as shown in Fig. 2. There were also two measurement stations into which two interchangeable units could be fitted. One of these was a Stanton-tube unit, as shown in Fig. 4, and the other was a heat-transfer unit, as shown in Fig. 5. These units could be bolted into the holes in the liner so that they were flush with the surrounding surface. There were seals to prevent air leaking up the sides of the measurement units from underneath the liner.

The Stanton-tube unit had one upstream-facing line of 3 Stanton tubes and another similar rearward-facing line. This was so that the skin friction could be measured where there was reversed flow near the surface in separated regions. Each Stanton tube was flanked by a pair of static holes. For strictly two-dimensional flow the static pressure would not vary across the tunnel, but in practice there were sometimes small transverse variations, and hence the static pressure appropriate to each Stanton-tube opening was taken to be the average of the readings of the two flanking static holes. The Stanton tubes were constructed as brass plugs which fitted tightly into three holes across the brass supporting disc. Each plug was made in two parts. The lower part had a conical depression in it and a central tapped hole, as shown in a detail of Fig. 4. Two sections were milled out of it to form the forward and rearward facing holes. The top of the plug was screwed hard into the bottom of the plug, and had a conical lower surface which mated with the corresponding surface in the bottom of the plug. Then the top was ground down until the lip thickness z was about 0·001 in. for tube A, 0·002 in. for tube B, and 0·003 in. for tube C. The finished plugs were pushed into the supporting disc and adjusted by means of the screws in the bottoms of the holes in the disc until the total height of the plugs above the surrounding surface was $2z$. Thus the lip thickness was equal to the opening, so that the tubes were all effectively geometrically similar. The actual total heights of the tubes above the surface were 0·0026 in., 0·0040 in. and 0·0062 in., the lip thicknesses being approximately half these values. After assembly Araldite was cast round the adjustment screws and hypodermic tubes where they emerged from the bottom of the supporting disc of the unit. This was to prevent air leakages from underneath the liner, where the pressure was typically about 4 in. of mercury absolute compared with about 2 in. on the top surface of the liner for a stagnation pressure of 30 in. Some air could also probably leak round the sides of the Stanton-tube plugs between the forward and rearward facing holes, but since the pressure differences were usually fairly small and the plugs were made to fit closely into the supporting disc, these leakages should be negligible. Two thermo-couples were mounted in the supporting disc of the unit.

The heat-transfer unit, interchangeable with the Stanton-tube unit, was constructed as in Fig. 5. In the centre was a brass 'thimble' whose top was flush with the surrounding surface but separated from it by a small air gap, the thimble diameter being 0·85 in. at the top, whilst the hole in the supporting disc was 0·87 in. in diameter. The thimble was held by the supporting disc on a ring of P.T.F.E., a material of low thermal conductivity. In the middle of the thimble there was a small electric bulb, and various voltages could be applied to it. The bulb was completely surrounded by metal, since the small brass disc into which the bulb was screwed butted up against the bottom of the thimble. A second outer 'guard box' of metal in thermal contact with the supporting disc surrounded the thimble as can be seen from Fig. 5. There was a sleeve of insulator material between the guard box and the thimble leaving small air gaps: this was to minimise convective heat transfer between the guard box and the thimble. Insulation on the outside of the guard box ensured that direct radiation from nearby fire elements did not heat it excessively. Thus it could reasonably be supposed that when the temperature of the top of the thimble was the same as the average temperature of the surrounding disc, the guard box would also be at this temperature and that there would then be no heat transfer between the guard box and the thimble. Hence the heat energy flowing out of the top of the thimble to the air stream would be equal to the wattage dissipated in the bulb. This wattage was determined by measuring the current through the bulb and the voltage across it. A thermo-couple in the centre of the top of the thimble measured the thimble temperature T_{th}, whilst four thermo-couples symmetrically situated in the supporting disc enabled the average temperature T_{av} of the disc to be determined. There was a static-pressure hole to one side in the supporting disc on a line through the centre perpendicular to the tunnel axis. At the same distance on the other side there was the mouth of a pitot-tube which could be moved by a micrometer underneath the tunnel in order to traverse the boundary layer. The pitot-tube had a 'shepherd's crook' form as shown in Fig. 5 so that readings could be obtained with it practically touching the wall. It was not quite parallel to the wall at its tip so that the underneath part of the tube at the tip was probably about 0·005 in. from the surface at the nearest position. The outside diameter of the tube was 0·070 in., and being made of stainless-steel hypodermic tubing it was sufficiently stiff not to bend appreciably in the wind.

Outside the tunnel the thermo-couple voltages were measured on a vernier potentiometer reading to one microvolt. The voltage and current for the heater bulb of the heat-transfer unit were measured similarly. The thermo-couple cold junctions, in glass tubes, were immersed in melting ice in a vacuum flask. Static pressures in the surface and Stanton-tube pressures were measured on a multi-tube barometer-type instrument. Each tube consisted of a U tube, one end of which was sealed with a Torricellian vacuum above the mercury. The difference in level of the mercury in the two limbs thus gave the absolute pressure. It was only necessary to read one limb since the bore of the tube was uniform, and the measurement scale was adjusted in height according to the room temperature to allow for effects of expansion on the mean level of the mercury. The reading was made with a barometer-type vernier, and the instrument was probably accurate to 0·005 in. of mercury. In contrast with some oil manometers, it was fairly quick to take up the pressure to be measured. Relatively high pressures, such as those in the boundary-layer pitot-tube, were measured on a conventional 30-in. mercury manometer.

The moisture content of the air in the tunnel was always quite low, frequent measurements of the dew-point being made to check this. Typically, for stagnation conditions of about one atmosphere pressure and a temperature of about 40 deg C, the corresponding frost point was about − 30 deg C.

4. *The Use of the Stanton-Tube Unit.* The Stanton tube may be calibrated in incompressible flow in, for example, a two-dimensional duct. The skin friction τ_w can be determined from the pressure drop along the duct. If the Stanton tube reads a pressure Δp higher than the static pressure, a suitable non-dimensional way of presenting the calibration data is, following Taylor[65] with slight modifications, to plot the ratio d'/d against R_s, where d is the height of the tube above the surrounding plate,

$$d' \equiv \left(\frac{2\Delta p}{\rho_w}\right)^{1/2} \frac{\mu_w}{\tau_w} \tag{6}$$

and

$$R_s \equiv \frac{\rho_w}{{\mu_w}^2} \tau_w d^2 \,. \tag{7}$$

The calibration curve can thus be expressed as

$$\frac{d'}{d} = F(R_s)\,. \tag{8}$$

In what follows, it is sometimes found convenient to refer to the quantity R_s as the 'Stanton-tube Reynolds number', although if τ_w is thought of as being $\rho_w\ U_\tau^2$, where U_τ is the friction velocity, $R_s = (\rho_w U_\tau d/\mu_w)^2$, and has the appearance of a Reynolds number squared. However, if τ_w is thought of as being viscosity times velocity gradient ($\mu\alpha$ in Taylor's[65] notation), R_s does have the appearance of a Reynolds number, and for a case where the upstream velocity profile is linear, R_s is the Reynolds number based on tube height d and the velocity at a distance d from the wall.

Wall values of the viscosity μ and density ρ have been specified in the definitions (6) and (7), although in incompressible flow μ and ρ are constant throughout the flow. However, with μ_w and ρ_w the definitions may also be used for compressible flow. For the tubes used in the present experiments d is taken as the total height (opening plus lip thickness) and thus is equal to $2z$ in the notation of Fig. 4. The relationship (8) between d'/d and R_s, found in the calibration experiment, is assumed to apply if the Stanton tube is used to measure the skin friction in the boundary layer. Then Δp is measured and ρ_w and μ_w are known so that τ_w can be deduced by, for example, assuming trial values of τ_w and finding the value which makes d'/d and R_s agree with the calibration. The validity of the assumption that calibration data found in, for example, a duct are applicable generally is discussed below. Meanwhile we note that if the velocity profile of the flow past the Stanton tube is linear with distance from the wall up to a distance d', then $d'\tau_w/\mu_w$ will be the velocity at d'. Since in incompressible flow $(2\Delta p/\rho_w)^{1/2}$ is the effective velocity measured by the Stanton tube, we can consider that the tube measures the velocity at d' from the wall, a distance which will be a function of Reynolds number R_s. However, the velocity distribution may not be linear for a distance d' and in these circumstances the tube does not measure the velocity at d', which is therefore best regarded merely as an effective measurement position.

Now consider a Stanton tube in the turbulent boundary layer on a flat plate. Assume that except in the laminar sublayer the velocity profile may be approximately represented by

$$\frac{u}{u_1} = \left(\frac{y}{\delta}\right)^{1/7}, \tag{9}$$

where δ, the boundary-layer thickness, is given by

$$\delta = 0 \cdot 38 x_e R_{xe}^{-1/5} \tag{10}$$

and x_e is the distance from the effective leading edge of the turbulent layer, R_{xe} being the corresponding Reynolds number. The relations (9) and (10) are roughly valid even for moderate supersonic Mach numbers. The skin friction,

$$\tau_w = \tfrac{1}{2}\rho_1 u_1^2 C_f = 0 \cdot 0296 \rho_1 u_1^2 f(M_1) R_{xe}^{-1/5}, \tag{11}$$

from equation (2), where $f(M_1) \equiv C_f/C_{fi}$, is a function of Mach number M_1 as given in Fig. 1. Thus very close to the wall in the inner part of the laminar sublayer

$$u = \frac{\tau_w}{\mu_w} y = 0 \cdot 0296 \frac{\rho_1 u_1^2}{\mu_w} y f(M_1) R_{xe}^{-1/5}. \tag{12}$$

The order of magnitude of the sublayer thickness t can be estimated by assuming that it is equal to that value of y for which relation (12) intersects relation (9), making the values of u equal. Hence from (10), if

$$\frac{\mu_w}{\mu_1} = \left(\frac{T_w}{T_1}\right)^{\omega},$$

$$t = (0 \cdot 0296)^{-7/6} (0 \cdot 38)^{-1/6} [f(M_1)]^{-7/6} \left(\frac{T_w}{T_1}\right)^{7\omega/6} R_{xe}^{1/10} \frac{\mu_1}{\rho_1 u_1}.$$

It follows from (7) and (11) that

$$\frac{d}{t} = (0 \cdot 0296)^{2/3} (0 \cdot 38)^{1/6} [f(M_1)]^{2/3} \left(\frac{T_w}{T_1}\right)^{(1/2)-(\omega/6)} R_s^{1/2}.$$

The exponent ω can be taken to be about $0 \cdot 9$ and $T_w/T_1 \simeq 1 + 0 \cdot 176 M_1^2$ for small rates of heat transfer. Hence, from Fig. 1 the product $[f(M)]^{2/3} (T_w/T_1)^{(1/2)-(\omega/6)}$ does not vary much with Mach number, being 1 at $M_1 = 0$ and about $1 \cdot 2$ at $M_1 = 3$. Accordingly

$$\frac{d}{t} \simeq 0 \cdot 09 R_s^{1/2} \tag{13}$$

for a boundary layer on a flat plate at free-stream Mach numbers in the range 0 to 3, and with small rates of heat transfer. This result is probably true also for incompressible turbulent duct or pipe flow, since the 'law of the wall' is much the same for all incompressible turbulent boundary layers.

Relation (13) shows that for R_s greater than about 30 the height d of the Stanton tube will be greater than half the sublayer thickness. Under such circumstances the results for the Stanton tube would not be expected to be the same when calibrated in turbulent flow as when calibrated in laminar flow. Nevertheless, different experimental calibration arrangements with turbulent flow would all be expected to give results roughly consistent with one another, because of the quasi-universality of the turbulent 'law of the wall', a point referred to again below. Further possible differences between laminar and turbulent calibrations may arise from the velocity and pressure fluctuations in the turbulent case, as Bradshaw, in a paper in preparation, has pointed out. His results, for a Stanton tube tested both in a laminar-flow duct and also in a turbulent-flow duct, show appreciable differences, as can be seen from Fig. 6, even though the biggest Reynolds number R_s investigated by Bradshaw with laminar flow was only about 20. Fig. 6 includes data for a number of different tubes tested by Bradshaw in turbulent flow, as well as a mean line through Hool's results[30] obtained in a laminar duct and a mean line through the turbulent calibration results of the present experiment, discussed later. Hool's results, obtained with a tube roughly similar to the smallest tube used by Bradshaw, agree quite well with the latter's laminar results. As for the turbulent results, since the tubes are not geometrically similar, it is not strictly legitimate to draw one curve through them, though in fact they all seem to lie close to one curve. This suggests that tube geometry is not very important, within reasonable limits. As against this, turbulent data from Stanton's original paper[63] give results for d'/d rather higher than Fig. 6. However, one has to take d equal to the opening of the tube in analysing Stanton's data, since the thickness of the lip is not given; if the results could be analysed taking d to be the opening plus lip thickness, they might agree better with Fig. 6. Be that as it may, it is evident from Fig. 6 that if it is intended to use the Stanton tube to measure skin friction in a turbulent boundary layer it is desirable to calibrate it also in turbulent flow. The calibration can then be regarded as a function of the quasi-universal 'law of the wall', exactly similar to the calibration of a Preston tube[50]. The flow near the measurement position in the calibration duct as used by Bradshaw and in the present experiments was not far from being two-dimensional, so the results should be closely applicable to measurements in boundary layers.

Although this procedure is satisfactory for incompressible flow, there are further difficulties when the flow is compressible. Compressibility effects would only be expected to be negligible if the Mach number near the tube was low, say, $M < 0\cdot5$ at a distance of two tube heights from the wall. In the present experiment for the attached boundary layer on the flat surface the values of R_s were in the range 40 to 200. Hence from (13) two tube heights would, for most of the cases investigated, be outside the sublayer. The boundary-layer thickness δ was roughly $0\cdot4$ in. at the upstream measurement position and $0\cdot7$ in. at the downstream position. Hence for the smallest tube, height $d = 0\cdot0026$ in., in the downstream position, $u/u_1 = 0\cdot497$ at a height of $2d$ if $u/u = (y/\delta)^{1/7}$ approximately. With a free-stream Mach number of about $2\frac{1}{2}$ and a small rate of heat transfer this means that approximately $M = 0\cdot88$ at $2d$. Similarly for the largest tube, for which $d = 0\cdot0062$ in., at the upstream position, $M = 1\cdot12$ approximately at $2d$. In these circumstances compressibility effects might clearly be important, so that straightforward application of the calibration data, obtained in incompressible flow through a duct, might lead to errors.

In an earlier investigation[18], one of us (Cope), using a Stanton tube whose height was adjustable, obtained results for skin friction in good agreement with Fig. 1 for conditions similar to those of the present experiment. The skin friction was deduced from the pressure measurements as follows: The velocity corresponding to the Stanton-tube reading was calculated in the standard way for reducing pitot-tube readings to velocities in compressible flow, on the assumption that the total temperature was constant across the boundary layer. Then this velocity was assumed to be the velocity at distance d' from the wall, where d' is as given by the incompressible calibration curve[8]; this matter is discussed above. To calculate R_s, trial values of τ_w had to be assumed. For the right value of τ_w the plot of velocity against distance from the wall, for the data obtained by traversing the Stanton tube, should be a smooth curve with a slope corresponding to τ_w at the wall. This procedure might lead to slightly different results for τ_w than would be obtained by applying equations (6), (7) and (8), but the discrepancies ought not to be more than 5 per cent. However, Cope did not calibrate the Stanton tube he used, but assumed the form suggested by Taylor[65] for the calibration function $F(R_s)$ of equation (8). This form asymptotes to $d'/d = \frac{1}{2}$ at large Reynolds numbers, as Stanton, in his original paper[63], assumed it would. However, there is no real reason to suppose that this must be so, and many of Stanton's own results correspond to lower values of d'/d. If the Stanton tube is allowed to be much higher than the sublayer thickness, very large Reynolds numbers R_s are obtained and very low values of d'/d, as can be seen from Fig. 6. Thus Cope assumed the calibration function $F(R_s)$ to be rather larger than it probably really should be at the fairly large Reynolds numbers at which he worked. The correct incompressible calibration curve would probably have given somewhat higher values of the skin friction, since if d'/d is assumed to be too large, τ_w is underestimated. As it happens the actual values for the skin friction obtained by Cope agree closely with Fig. 1, but this may well be due to a fortunate cancellation of opposing errors.

To obtain quantitatively accurate results with a Stanton tube in compressible flow it ought to be calibrated in compressible flow. This is difficult to do. Abarbanel, Hakkinen, and Trilling[1] compared the readings of a type of Stanton tube with direct force measurements obtained with a floating element at Mach numbers between 1·33 and 1·87. However, their tube was in fact a flattened pitot-tube close to the surface, so its calibration would differ from that of a more conventional Stanton tube.

In the present experiments the tubes were calibrated in incompressible flow. It was hoped to be able to correct for the compressibility effects by the use of three tubes of different heights, whose calibration results in incompressible flow should lie on a single curve because the tubes were geometrically similar. It was thought that when the incompressible calibration was applied to the readings in compressible flow, different estimates for the skin friction τ_w would be obtained from each tube. If these values were then plotted against tube height, and the curve extrapolated to zero height, the correct value of τ_w could, it was hoped, be estimated. In practice, however, the values of τ_w for the three tubes showed little consistent trend with tube height: the intermediate-height tube tended to read lowest and the smallest tube highest. It seems unlikely that the average τ_w values for the three tubes are the correct ones, since they are about 15 per cent higher than estimates obtained from the momentum equation, and about 25 per cent higher than the generally accepted figures. It may be that there is a compressibility effect which is very non-linear with tube height, and reaches a sort of plateau. In this connection it is perhaps significant that the Mach number at twice the tube height, as estimated above, varies comparatively little for wide variations in the ratio of the tube height d to the boundary-layer thickness δ.

The actual incompressible calibration results for the Stanton tubes used in the present experiment are shown in Fig. 7. The calibration was done in a duct, as used by Bradshaw and Gregory[6]. The working-section dimensions were 2 in. by 12 in., and there was a 24-ft long entry section ahead of the working-section where accordingly the flow approximated to fully developed turbulent channel flow. Allowances were made for the finite width of the channel so that the skin friction at the position where the Stanton tubes were inserted, at the centre of the 12 in. walls of the working-section, was known. The calibration was done both before and after the experiments in the supersonic tunnel to make sure that no changes occurred. The points are more scattered than those of Fig. 6, for which a more sensitive manometer was used, but a reasonable mean curve is

$$\frac{d'}{d} = cR_s^{-1/4} \text{ with } c = 1\cdot 7 \,. \tag{14}$$

This curve also fits some results, not shown in Fig. 7, obtained by calibrating the Stanton tubes of the present experiment in a duct resembling that used by Hool. The duct was 0·050 in. high and 4 in. wide, and was clamped on to the top of the flat liner with the Stanton tube unit in position. Despite the small height of this duct, the flow in it was probably only laminar for the lowest Reynolds numbers. Relation (14) is shown on Fig. 6, and can be seen to be quite close to Bradshaw's results obtained with tubes of different shape.

From (6), (7) and (14), if viscosity is assumed to vary approximately as (absolute temperature)$^{0\cdot 9}$, convenient formulae can be obtained for deducing the skin friction τ_w from the Stanton-tube readings. The formulae relate τ_w to the Stanton-tube excess pressure Δp and the static pressure p, in inches of mercury, to the tube height d in thousandths of an inch, and to the wall temperature T_w deg K, and are as follows:

$$\frac{\tau_w}{p} = 0\cdot 998 \times 10^{-2}\left(\frac{2}{c}\right)^{4/3}\left(\frac{30}{p}\right)^{2/3}\left(\frac{T_w}{288}\right)^{2\cdot 8/3}\left(\frac{\Delta p}{pd}\right)^{2/3} \tag{15}$$

$$= 1\cdot 240 \times 10^{-2}\left(\frac{30}{p}\right)^{2/3}\left(\frac{T_w}{288}\right)^{2\cdot 8/3}\left(\frac{\Delta p}{pd}\right)^{2/3} \text{ with } c = 1\cdot 7$$

$$C_f = \frac{1\cdot 426 \times 10^{-2}}{M_1^2}\left(\frac{2}{c}\right)^{4/3}\left(\frac{30}{p}\right)^{2/3}\left(\frac{T_w}{288}\right)^{2\cdot 8/3}\left(\frac{\Delta p}{pd}\right)^{2/3} \tag{16}$$

$$= \frac{1\cdot 771 \times 10^{-2}}{M_1^2}\left(\frac{30}{p}\right)^{2/3}\left(\frac{T_w}{288}\right)^{2\cdot 8/3}\left(\frac{\Delta p}{pd}\right)^{2/3} \text{ with } c = 1\cdot 7 \,.$$

In equation (16), M_1 is the Mach number at the edge of the boundary layer. It is not practicable to specify this in separated regions, where accordingly τ_w/p is a better non-dimensional measure of skin friction than C_f.

5. *The Use of the Heat-Transfer Unit.* The energy generated in the bulb in the heat-transfer unit flowed partly out of the top of the thimble to the air stream and partly in other directions. This latter 'leakage' heat flow could reasonably be supposed to be zero (as pointed out in Section 3), if the temperature T_{th} of the top of the thimble were equal to the average, T_{av}, of the temperatures recorded by the four thermo-couples in the supporting disc. Hence when T_{th} differed a little from T_{av} the energy balance would be as follows:

$$\text{Heat flow } H \text{ from top of thimble to stream} = \text{Watts, } W\text{, generated in bulb} + C(T_{av} - T_{th}) \,, \tag{17}$$

where C is a constant depending on the geometry of the unit and the thermal conductivity of the materials used in its construction. It is now necessary to decide how H will vary with T_{av} and T_{th}.

Consider firstly a body whose surface temperature T_w is uniform. The heat transfer between surface and stream at any particular point on the body will vary with T_w, and for a certain temperature, the effective recovery temperature T_{re} for that point, it will be zero. For T_w not very different from T_{re} the rate of heat transfer per unit area from wall to stream at the point can be expressed as $h(T_w - T_{re})$. As explained by Eckert and Livingood[24] and Korobkin[35], T_{re} may not be constant over the surface of the body. It will be approximately constant if the body is a flat plate with turbulent flow from close to the leading edge, but if the body has a stagnation point, for example, T_{re} will vary with position. In this event T_{re} is not necessarily the same as the local recovery temperature for a geometrically similar body made of a perfect thermal insulator. Likewise the heat transfer will not be equal to $h(T_w - T_{re})$ if the wall temperature, instead of being uniform, varies with position and is only locally equal to T_w. Despite this, h and T_{re} as determined in experiments on bodies at uniform temperature are quantities of practical interest. For one thing, the case of a body at uniform temperature may well arise in practice. It corresponds, for example, to conditions when a body is first set in motion, though of course in such a case at high Mach numbers $(T_{re} - T_w)$ may be so large that the heat-transfer rate is no longer a linear function of it. In the second place, even if the body temperature does vary with position, the local heat-transfer rate will probably not be far from $h(T_w - T_{re})$ if T_w does not vary too sharply. In the present experiment the surface temperature in the vicinity of the heat-transfer unit was roughly uniform (typically about 65 deg C). Hence, if the temperature T_{th} of the thimble were equal to the average temperature T_{av} of the adjacent surface, the rate of flow of energy from the top of the bulb to the stream could be expressed as $hA(T_{av} - T_{re})$, where A is the area of the top of the thimble and is equal to 0·567 sq in. The temperature differences $(T_{av} - T_{re})$ were normally about 45 to 50 deg C with T_{re} about 18 deg C, so it could be assumed that the heat transfer would vary linearly with $(T_{av} - T_{re})$. Hence the energy-balance equation (17) would become

$$H = hA(T_{av} - T_{re}) = W. \tag{18}$$

A possible way of using the instrument would have been to have adjusted the voltage to the bulb until, after allowing time for steady conditions to become established, T_{th} was equal to T_{av}. Then equation (18) would apply. The unknown T_{re} could be eliminated by repeating the process with a different current in the heater bars under the liner to give a different average temperature. In practice, however, it was more convenient to proceed as follows: After establishing steady conditions with no current in the heater bars or in the bulb of the heat-transfer unit, T_{th} and T_{av} were determined: these values may be written T_{0th} and T_{0av}. Even for the flat surface T_{0th} was not equal to T_{0av} in general. This was because there was some heat transfer to the stream associated with a flow of heat along the liner. This flow was from the region near the throat, where the metal tended to take up almost the full stagnation temperature, to the downstream end, which tended to take up the recovery temperature appropriate to a Mach number of about $2\frac{1}{2}$. Measurements were also made with the liner heated. The current in the heater bars was kept approximately constant, and after sufficient time to establish steady conditions, T_{th} and T_{av} were found for various wattages W in the bulb. After changing W it was necessary to wait about a quarter of an hour before conditions steadied. This was much shorter than the steadying time required if any major change were made in the current through the heater bars. The wattages W were not in general such as to make T_{th} and T_a equal, and hence the relation (18) for the heat flow H between the top of the thimble and the stream could not be expected to apply. It was assumed instead that

$$H = hA(T_{th} - T_{re}) + D(T_{th} - T_{av}), \tag{19}$$

where D depends on the position of the measurement station and on the nature of the flow but not on the general level of temperature T_{av}. If the diameter d of the top of the element were sufficiently small compared with the effective length of run of turbulent boundary layer upstream of it, the analyses of Ludweig[39] or Liepmann and Skinner[37] show that D in equation (19) could be represented by

$$D = EAk_w \left(\frac{\rho_w \tau_w}{\mu_w^2 d}\right)^{1/3} - hA ,$$

where E is a constant and k_w is the thermal conductivity of air at the wall. The product $k_w(\rho_w/\mu_w^2)^{1/3}$ is very insensitive to wall temperature and so is $\tau_w^{1/3}$, so that (19) would be justified. Comparison with the work of Rubesin[54] suggests that (19) is also valid for larger values of d, when D in (19) would depend simply on the ratio of d to the effective length of run of turbulent boundary layer upstream of the element.

It follows from (19) and (17) that

$$hA(T_{th} - T_{re}) = W + L(T_{av} - T_{th}) ,$$

where L is a constant. For no current in the heater bars or in the bulb of the heat-transfer unit

$$hA(T_{0th} - T_{re}) = L(T_{0av} - T_{0th}) . \tag{20}$$

Hence

$$hA(T_{th} - T_{0th}) = W + L[T_{av} - T_{th} - (T_{0av} - T_{0th})] . \tag{21}$$

It has been tacitly assumed here that during a run no variations occurred in the tunnel stagnation temperature T_s. In practice there were small variations, usually less than about 1 deg C. It would be expected that T_{re} would vary by about the same amount as T_s. Hence in place of (21) we should write

$$hA(T_{th} - T_{0th} - T_s + T_{0s}) = W + L[T_{av} - T_{th} - (T_{0av} - T_{0th})] , \tag{22}$$

where T_s is the stagnation temperature at the time when T_{th}, T_{av}, and W were measured and T_{0s} is the stagnation temperature when there was no current in the heater bars and bulb.

From the measured values and equations (22) and (20), h and T_{re} could be found. For each wattage W a straight line of L against hA could be plotted such that the co-ordinates satisfied (22). For a given flow and measurement station, the different straight lines corresponding to the different wattages W should all have intersected at one point. They did so approximately as can be seen from Figs. 8 and 9, which show typical intersections obtained. The intersection point was judged by eye. This gave L and hA. Then the effective recovery temperature T_{re} corresponding to the stagnation temperature T_{0s} could be found from (20). An effective recovery factor r_e could also be calculated such that

$$\frac{T_{re}}{T_{0s}} = \frac{1 + 0{\cdot}2 r_e M_1^2}{1 + 0{\cdot}2 M_1^2} , \tag{23}$$

where M_1 is the free-stream Mach number, approximately 2·44. The experimentally determined values of L did not vary much, being in the range 0·17 to 0·22 watts per deg C. This means that the thermal conduction term C of equation (17) was much bigger than the factor D of equation (19).

In terms of conditions at the edge of the boundary layer, a Stanton number can be defined in the normal way as

$$St = \frac{h}{\rho_1 C_p u_1} .$$

From this it can be shown that, if h is in watts per square inch, deg C,

$$St = 3 \cdot 69 \times 10^{-3} \left(\frac{30}{H_0}\right) \left(\frac{T_s}{288}\right)^{1/2} \frac{(1 + 0 \cdot 2M_1^2)^3}{M_1} h \,, \tag{24}$$

where the stagnation pressure H_0 is in inches of mercury and the stagnation temperature T_s is in deg K. It has been assumed in deriving this relation for St that the external flow is isentropic. This is not true in separated regions, but there conditions at the edge of the boundary layer are uncertain and the concept of Stanton number loses its usefulness.

6. *The Results for the Flat Surface.* Table 1 shows results for the Stanton number and effective recovery factor as determined from the readings of the heat-transfer unit, and for the skin friction as determined from the readings of the Stanton-tube unit. Results were obtained at the two measurement stations (*cf.* Fig. 2) for three different stagnation pressures H_0. Skin-friction results are not presented for the earlier runs, because the type of Stanton-tube unit used then was unsatisfactory. The heat-transfer measurements made in the earlier runs at the forward measurement station gave higher results for the Stanton number than the results obtained later, but the reason for this is not known. Skin-friction values are shown in Table 1 for the tubes A, B, and C of different heights (*cf.* Fig. 4), but as discussed in Section 4 above, it is not clear what compressibility effects are associated with the different tube heights. Stanton-tube readings were taken when the liner was unheated and also when it was heated. It can be seen from the Table that surface temperature has little effect on skin friction. The Stanton-tube excess pressure Δp was reduced as the wall temperature T_w was increased, and the net effect on the result for C_f as estimated from equation (16) was small.

Figs. 10 and 11 show the Mach-number profiles through the boundary layer for the two measurement stations at the three different stagnation pressures. The Mach number was calculated from the pitot pressure on the assumption that the static pressure was constant across the boundary layer. Results obtained for nominally the same flow conditions on different dates show small differences but mean curves have been drawn through the points. The profiles obtained when the liner was heated differ slightly from those for the unheated liner, the unheated profiles being fuller with less total thickness. From the average Mach-number profiles for the unheated cases the momentum thicknesses θ and effective total thicknesses δ have been estimated. For calculating θ the total temperature was assumed constant across the boundary layer. This is not quite accurate but should lead only to small errors in θ. For estimating δ, the relatively straight sloping part of the profile was extrapolated to intersect at an angle the line $M = M_1$, where M_1 is the Mach number at the edge of the boundary layer. Thus the extrapolated Mach-number profile resembled the conventional 'power law' velocity-profile representation and δ was correspondingly taken to be y at the corner. Results are shown in Table 2, which includes values of θ/δ. For a fifth-power velocity profile with constant total temperature at a Mach number of $2 \cdot 44$, $\theta/\delta = 0 \cdot 0817$, whilst for a seventh-power profile it is $0 \cdot 0705$ (*cf.* Refs. 19 and 68). The results for θ/δ in Table 2 lie between these values, indicating that the experimental profiles approximated to power-law profiles of index between $^1/_5$ and $^1/_7$.

As discussed in the introductory Section 1, St and C_f may be related to the corresponding quantities for incompressible flow over a flat surface. From equations (1), (2) and (4)

$$\frac{C_f}{C_{fi}} = \left(\frac{C_f}{0 \cdot 0259}\right)^{4/5} R_\theta^{1/5} \,,$$

$$\frac{St}{St_i} = \left(\frac{St}{0 \cdot 0155}\right)^{4/5} R_\theta^{1/5} \,.$$

Table 3 and Fig. 1 show the average results from Table 1 compared on this basis, the skin-friction data being those for the unheated liner. The results for St/St_i are roughly in agreement with Fig. 1, but the values for C_f/C_{fi} are rather higher, though still of the right order. The ratio St/C_f is correspondingly less than the usual value of about 0·6; instead, according to the figures of Table 3 it is in the region of 0·42 to 0·45. The experimental recovery factors of Table 1 are mostly slightly below the usual value of between 0·88 and 0·89. One high value of 0·905 was obtained, but it is thought that insufficient time had been allowed in this case for complete thermal equilibrium to become established.

The anomalous results for skin friction are probably due to compressibility effects on the Stanton-tube readings, as discussed in Section 4. It is not surprising that the relations (15) and (16), which express the incompressible calibration results for the Stanton tube, should give values for the skin friction which are too high. Better results might be obtained if, in place of using the wall temperature T_w in the formulae, some kind of average temperature for the region of flow influenced by the tube were used. In compressible flow this 'effective T_w' would be less than T_w, and hence would give smaller skin-friction results. However, it is not easy to decide what best effective T_w to take, and how it would vary with tube height.

An independent estimate of skin friction may be obtained from the momentum-thickness results. The momentum equation for compressible flow may be written

$$C_f = \frac{2d\theta}{dx} + 2\theta\left\{\frac{(2 + H - M_1^2)}{M_1\left(1 + \frac{\gamma - 1}{2} M_1^2\right)} \frac{dM_1}{dx}\right\},$$

where $H \equiv \delta^*/\theta$, the ratio of the displacement to the momentum thickness. In the present experiment, downstream of the position A shown in Fig. 2 the pressure was nominally constant, but even if dM_1/dx had not been zero everywhere, the contribution of the second term on the right-hand side of the momentum equation would have been small. This is because $(2 + H - M_1^2)$ is small for a 'flat plate' turbulent boundary layer at a Mach number M_1 of approximately 2·44 (*cf.* Ref. 68). Hence the skin-friction coefficient at a position roughly half way between the two measurement stations should be equal to $2\Delta\theta/\Delta x = C_f'$, where $\Delta\theta$ is the increase of θ and Δx, equal to 19·75 in., is the distance between the two stations. For $H_0 = 30$ in., 20 in. and 13 in. of mercury respectively, $C_f' \times 10^3 = 1{\cdot}98$, 2·16, and 2·34. Assume that the momentum thicknesses appropriate to these values C_f' are the averages of those measured at the upstream and downstream stations. Then the appropriate values of R_θ are 9945, 6995, and 4840 and accordingly $C_f'/C_{fi} =$ 0·806, 0·804, and 0·802.

The results for C_F/C_{Fi}, where C_F is the coefficient of average skin friction, agree closely with those for C_f'/C_{fi} if the effective origin of the turbulent boundary layer is assumed to be at such a position that the values of C_F/C_{Fi} agree for the two measurement stations. The distances of this effective origin, so estimated, upstream of the forward measurement station are 22·7, 21·6 and 21·0 inches for stagnation pressures of 30, 20 and 13 inches of mercury. These positions are about 8 inches downstream of the throat, as is reasonable because of the favourable pressure gradients near the throat.

Although the values for C_f'/C_{fi} and C_F/C_{Fi} are lower than those given by the Stanton-tube measurements, they still lie a little above the curve of Fig. 1. Nor could the results for C_f'/C_{fi} be made to agree with Fig. 1 by making small adjustments to the assumed values of R_θ, since C_f/C_{fi} is proportional to the fifth root of R_θ. As mentioned in the Introduction, the momentum-thickness method of estimating C_f is quite likely to give results that are a little too high in supersonic flow, because of the neglect of the turbulent normal stresses. Also, of course, it may be that the skin friction in our experiment was really slightly higher than it would have been if the pressure had been constant right from the leading edge. Nevertheless, it is clear that due presumably to compressibility effects, the Stanton-tube results for skin friction are too high by a significant, though not large, amount.

When the pitot-tube used for traversing the boundary layer was practically touching the wall it was effectively a Preston tube[50]. As mentioned in Section 3, there was a gap of about 0·005 in. between the wall and the bottom of the tube at its nearest position to the wall. The tube diameter was 0·070 in., so it could be regarded roughly as a tube of, say, 0·073 in. effective diameter d in contact with the wall. The pressure P recorded by the pitot-tube at this position was known, as was the static pressure p, so that following Preston[50] we could plot $\log_{10}(\tau_w d^2/4\rho\nu^2)$ against $\log_{10}[(P - p)d^2/4\rho\nu^2]$, where average values of the Stanton-tube estimations, corresponding to the skin-friction-coefficient values in Table 3, were taken for the skin friction τ_w, and the fluid properties ρ and ν were evaluated at the wall. The results approximated to the line

$$\tau_w d^2/4\rho\nu^2 = 0\cdot054[(P - p)d^2/4\rho\nu^2]^{0\cdot85}\,. \qquad (25)$$

The numerical coefficient 0·054 on the right-hand side would have been reduced, had lower values of the skin friction been used, to correspond with the momentum-thickness estimations. For incompressible flow over a flat plate it has been found[51] that

$$\tau_w d^2/4\rho\nu^2 = 0\cdot0457[(P - p)d^2/4\rho\nu^2]^{0\cdot875}\,. \qquad (26)$$

Although this is formally little different from (25) it indicates higher values of $\tau_w d^2/4\rho\nu^2$ for given values of $(P - p)d^2/4\rho\nu^2$ in the region of 10^6, as in the present experiment. Thus if we had attempted to determine the skin friction using the Preston tube in conjunction with the incompressible calibration, we should have obtained estimates even higher than the Stanton-tube results. This is clearly because a Preston tube of the size used in the present experiments is subject to considerable compressibility effects. These effects are, as would be expected, of the same sign as, and bigger than, the effects on the Stanton-tube readings.

7. *The Results for the Separated Regions.* Fig. 12 shows results obtained through the separated regions for the pressure p at the wall, the ratio of the viscous stress τ_w at the wall to p, the heat transfer h, as discussed in Section 5, in watts per square inch, deg C, and the effective recovery factor r_e as defined by equation (23) with $M_1 = 2\cdot44$. Fig. 13 shows Mach-number profiles at various stations in the separated regions. The Mach number was calculated from the pitot pressure on the assumption that the static pressure was equal to the value it had at the wall. Traverses were accordingly terminated where it was obvious in the schlieren picture that the tip of the pitot-tube was about to enter any region where there were sharp pressure gradients. Thus the traverses were not, for example, continued through the compression waves that can be seen in Fig. 3. The results are subject to some errors since the pitot-tube was approximately parallel to the wall and so was at a considerable angle to the flow at some positions. The pitot-tube pointed forwards and hence did not give the Mach number in regions where the flow was reversed. In such regions in Fig. 13 the profiles have accordingly been shown dotted, to indicate that the true profiles would probably have been different.

The pressure distributions in Fig. 12 show no very unusual features. The overall pressure distributions were very little different when the wall was heated from what they were when the wall was unheated, though as mentioned in the previous Section, there were detectable differences in the boundary-layer profiles for the flat surface. Ahead of the front step in Fig. 12 the pressure rises steeply to a plateau, then dips a little, and close to the step increases again. If the pressure could have been measured right in the corner it would probably have been found to be considerably higher than the plateau pressure (*cf.* Ref. 33). The dip in pressure and rise in the corner is thought to be associated with a strong vortex in the corner. The schlieren photograph of Fig. 3 shows evidence of pressure gradients near the corner, and these gradients probably invalidate the Mach-number profile in Fig. 13 for the position closest to the front step.

Downstream of the rear step the pressure is constant at a low value close to the step. The ratio of this pressure to the free-stream pressure is about 0·30, whereas the usual turbulent base-pressure ratio for a Mach number of 2·44 is about 0·24 (*cf.* Ref. 29). However, the boundary layer just upstream of the base is more than usually thick compared with the base height in the present instance, and this could account for the discrepancy. Downstream of the base-pressure region, the pressure rises steadily and approaches the free-stream value.

The skin friction at the wall well upstream of the front step has the same value that it has in the absence of a step. At the point where the pressure begins to rise the skin friction falls, and becomes zero at a position where the ratio of the pressure to its free-stream value is about 1·82, so that the pressure coefficient at separation is about 0·20. This agrees with the results of Ref. 29. Downstream of separation the skin friction becomes negative and fairly small, but close to the step it becomes larger and negative. Fig. 12 shows τ_w/p, and p is bigger near the step than upstream, so that the maximum negative value of τ_w is not far short of half the upstream value in magnitude. There is clearly a more intense reversed flow close to the step, probably associated with the vortex mentioned above.

Further evidence of this is provided by the oil-flow photographs of Fig. 14. These were obtained by smearing oil containing a white pigment on the surface. When the flow was established the oil was teased out into filaments in regions where the skin friction was large. This can be seen in the region well upstream of the step in (a) and (b) of Fig. 14. The circle marks the edge of the heat-transfer unit where there was a slight crack in which oil collected. While the oil tests were being done a band of Sellotape was stuck over the top of the unit to prevent oil getting inside it, and the edge of this Sellotape is visible. Just downstream of the heat-transfer unit the filament lines terminate in a line parallel to the step, and $4\frac{1}{2}$ inches upstream of it. It is thought that oil accumulates at the point where the pressure begins to increase: the skin friction is still not zero or reversed here, but the accumulation of oil remains at rest because the increased pressure on its downstream side tends to push it upstream whilst the skin friction tends to push it downstream. A little downstream of this well-marked transverse line there is a less well-marked band of oil that appears not to have been moved at all. It is thought that this is where separation occurs, since it agrees with the position at which the measured skin friction as shown in Fig. 12 is zero. Downstream of separation the oil is moved in the upstream direction in little waves, suggesting that the reversed flow is not very intense. However closer to the step filaments occur, extending in Fig. 14b over a distance of about $1\frac{1}{2}$ inches from the step. Photograph (b), taken while the tunnel was running, shows that these filaments have moved upstream relative to photograph (a), which was taken at an earlier instant. This clearly shows the reversed skin friction close to the step, and the most reasonable explanation is that there is a vortex whose core is situated close to the step, so that the reversed flow is most intense there, as sketched in Fig. 15a. There may be a small secondary vortex of opposite sign right in the corner, as in Fig. 15b, since in Figs. 14a and 14b there can be seen a band of oil on the forward face of the step parallel and close to the corner. On the other hand there is no sign of this supposed secondary vortex on the liner upstream of the step. Hence, it may be that the line of oil on the forward face is analogous to the well-defined transverse line just upstream of separation on the liner, and is associated with a steep pressure gradient on the face of the step close to the corner. Kepler's and Bogdonoff's results[33] for the pressure distribution on the face of a forward-facing step are consistent with this, since they found the pressure to be relatively high at the corner with a minimum at rather less than half way up the step, a type of pressure distribution which agrees with the schlieren photograph (Fig. 3).

Behind the rear step the oil flow photographs (c) and (d) of Fig. 14 show a region of undisturbed oil extending up to about 1 in. from the step, and then a region of reversed flow followed by a second band of quiescent oil, whose edges are roughly at 1·95 in. and 2·35 in. from the step. Downstream again the oil is teased out in the same direction as the main flow. The skin-friction measurements of Fig. 12 show virtually zero results up to a distance of 1·8 in. from the step, as discussed further below, and then the skin friction increases. If reattachment occurs at about 1·8 in. (which is consistent with the Mach-number profiles of Fig. 13), it means that the second band of unmoved oil in Figs. 14c and 14d is a little downstream of reattachment. This might be so because of the possible action of the pressure gradients on the oil tending to push it upstream. Thus the oil would perhaps remain still at points where there was a positive skin friction tending to push the oil downstream against the pressure gradients. The pressures at the edges of the band of still oil, 1·95 in. and 2·35 in. from the step, can be seen from Fig. 12 to be 0·88 in. and 1·12 in. of mercury. Hence the increase of pressure divided by the mean pressure is 0·24. At the middle of the band of still oil τ_w/p is about 3×10^{-3}. Hence the oil layer would have to be 5 thousandths of an inch thick for the pressure force acting on it to balance the friction force of the air. This thickness is possible. Also, of course, any very small out-of-balance force on the oil would not move it appreciably in the limited time for which the airflow is maintained over the oil. It is not surprising that the band of oil downstream of reattachment is more diffuse than the hard line of oil just upstream of separation ahead of the forward step, because in that case the oil probably piles up into a thicker accumulation, and the pressure gradients and skin friction are bigger.

The reason for the reversed flow of oil behind the rear step between the two bands of still oil is not clear. The skin friction has been shown in Fig. 12 as zero up to 1·8 in. from the step, but in fact the Stanton-tube readings were equivocal. At about 0·8 in. from the step the two outermost reversed Stanton tubes gave readings the same as or slightly less than the corresponding static pressures, whilst the centre tube read a pressure slightly higher than the corresponding static pressure. At about 1·8 in. from the step one of the reversed Stanton tubes read lower than the static pressure whilst the other two read higher. A partial explanation for these discrepancies between the various tubes is that the pressure and skin friction are low close to the rear step, so that pressure differences are small and difficult to measure. (These considerations also account for the large scatter on the readings where the skin friction begins to rise downstream of reattachment.) However, it is thought that not all the discrepancies between the tubes in the region of separation can be accounted for in this way. The residual real effects may be due to small spanwise variations in pressure, though the oil-flow pictures show that the flow is reasonably two-dimensional. Since on the average the readings at 1·8 in. from the step show more sign of reversed flow than those at 0·8 in., it may be that there is a region of small reversed skin friction away from the step where the oil flow is reversed, but that the skin friction is virtually zero closer to the step. This could account for the oil pattern. It would imply that the flow must be as shown in Fig. 16a, with a vortex whose core stands away from the step, and possibly a slow secondary vortex of opposite sign in the corner. It is not clear why there should be this difference from the forward-facing step, and an alternative explanation is that the skin friction is indeed virtually zero up to reattachment, with a weak vortex as in Fig. 16b, but that the oil pattern is governed by the pressure distribution. On this view the reversed flow of oil would be due principally to the pressure gradient, and would terminate where the pressure becomes constant at the base pressure. The pressure begins to rise above the base pressure at about 1·3 in. from the step, whereas the band of still oil extends only to 1 in. from the step, so there would presumably have to be some residual action of the small reversed skin friction.

Whatever the actual flow pattern may be, it is clear that after a short region of low, probably reversed, skin friction, the skin friction increases steadily, but does not reach the value it would have in the absence of a step till at least eight step heights downstream of the step. It should be noted that Fig. 12 shows τ_w/p, so that τ_w increases less rapidly downstream of reattachment than does τ_w/p.

Perhaps the most surprising results of Fig. 12 concern the heat transfer. The quantity h shown is, as discussed in Section 5, the heat transfer in watts per square inch divided by the difference in deg C between the surface temperature and the local effective zero heat-transfer temperature T_{re}. The measured values of h represent mean values over the top of the thimble of the heat-transfer unit, and not true point values. Hence, if there were any sharp variations in h over a distance less than the diameter, 0·85 in., of the thimble, they would not be detected accurately.

It can be seen from Fig. 12 that upstream of the front step h starts off a little below the value it would have in the absence of a step. Probably it ought to be the same, but there may be small errors due to heat flows introduced by local longitudinal temperature gradients. As the step is approached, h at first increases, then decreases again, and finally increases till near the step it is about twice its upstream value. When the surface temperature T_w, assumed roughly uniform, is very different from T_{re}, the variations from point to point in T_{re} make little difference to $T_w - T_{re}$. Hence then the actual heat transfer per unit area is proportional to h, provided that $T_w - T_{re}$ is not so large that the heat transfer is no longer a linear function of it. In the present case, however, there were appreciable proportional variations in $T_w - T_{re}$. Hence if the wattage to the bulb in the heat-transfer unit had been adjusted to make the thimble temperature T_{th} equal to the average temperature T_{av} of the adjacent surface, this wattage, and the corresponding heat transfer per unit area, would not have been twice as great near the front step as upstream. Nevertheless, they would have been somewhat greater there as can be seen from Table 4. For this Table the wattage W for which T_{th} would have been equal to T_{av} was obtained by cross plotting $T_{th} - T_{av}$ against W, and the corresponding values of T_{av} and of the stagnation temperature T_s were similarly determined.

Table 4 includes results for the rear step as well as for the front step, and it can be seen that in the region of reattachment and downstream the wattages are appreciably greater than they would be in the absence of a step. Likewise h in Fig. 12 is greater. Close to the step, however, h is small. These findings agree qualitatively with those of Bernard and Siestrunck[2] and Naysmith[47]. In the present experiments, the effective negative value of W in Table 4 for the position closest to the rear step arises because even with no current to the bulb the thimble of the heater unit was slightly hotter than the surrounding plate when the liner was heated by the heater bars. Perhaps the circulating 'dead' air came to the position of the thimble with a temperature slightly higher than the local value of T_{av}. There were some variations in T_{av} from point to point as can be seen from Table 4, though the variations there may partly be due to the fact that the readings were taken on different days, so that the room temperature and, probably, the currents in the heater bars, were not always the same. The low value of T_{av} for the position 2·46 in. behind the rear step was due to the rearmost heater bar being broken on the day those results were taken, so that the rear end of the liner was not quite as warm as usual. Before the next run the heater bar was replaced. Thus several factors tended to cause variations in the surface temperature, but besides those just mentioned there probably were at any one time residual spatial variations due to the disposition and characteristics of the heater bars and the differences in the rates of heat transfer from point to point. It seems likely from Table 4 that the average temperature of the wall behind the rear step as far as reattachment was higher than the local temperature close to the step, and this could account for the circulating air being at a higher temperature than T_{av} close to the step, and hence for the negative value of W in Table 4. On this interpretation negative effective values of W could not have occurred if, apart from the thimble of the heat-transfer unit, the wall temperature had been perfectly uniform everywhere. Probably also h in Fig. 12 would not have been negative (though small) close to the rear step. For in cases in which the wall is hot, as in the present experiment, the total temperature of the gas would not normally exceed the wall temperature anywhere. However, it would have to do so if h were negative, because negative values of h would imply temperature gradients in the air such that at a small distance from the wall the temperature would have to be higher than at the wall. This seems very unlikely because in an ordinary boundary layer with a hot wall not only the static temperature, but even the total temperature of the moving fluid is less than the temperature of the wall. Admittedly the boundary-layer approximations may not be valid in a separated region, and it is possible to think of flows where the temperature is a minimum at points of minimum velocity. Thus Bernard and Siestrunck[2] cite the case of a vortex in 'solid body' rotation where no heat is generated by friction and where in turbulent flow the temperature would probably be related to the pressure by the relations for an adiabatic compression, being greatest at the periphery. However, though this may be relevant to the problem of the Ranque or Hilsch tube, it does not seem relevant to the present situation, where the region of interest is the boundary of the circulatory flow and where in any case the dynamic forces are small. The cases investigated by Ryan[56] might at first sight seem to be more pertinent. His experiments concerned the flow at transonic speeds past bluff bodies, where wakes of the 'vortex-street' type occurred, and he found that for zero heat transfer to the body the time-average of the total temperature in some regions of the flow was a good deal less than the stagnation temperature, whilst in other regions it was higher. However, these effects seem to be confined to cases, such as vortex-street wakes, which are unsteady but possess a certain regularity. The flow pattern in the present experiments is steady on a large scale, though of course there are small-scale turbulent eddies. Spatial variations of total temperature on the scale of the turbulent eddies would not, however, be detected by the relatively large-sized instruments used, and in any case they would be random. Hence it seems likely that for a truly uniform surface temperature the heat transfer would not be negative anywhere, though it might well be zero close to the rear step.

The high rates of heat transfer ahead of the front step and near reattachment downstream of the rear step remain to be accounted for. It might be thought that conditions just in front of the forward step were associated with a possibly high rate of heat transfer at the top of the step where the flow reattaches. Then the effects of this might be conducted round through the metal. However, this cannot be the true explanation, since the heat-transfer unit measures the local interchange between the wall and the flow. Hence, provided the step were maintained at roughly the same temperature as the liner upstream, the heat transfer just upstream of the step would not be affected if a layer of thermal insulator were inserted between the step and the liner, as sketched in Fig. 17.

The theoretical work of Chapman[13] throws some light on the situation. Chapman found that for extensive separated flows with thick regions of nearly dead air, the average heat transfer at the surface between separation and reattachment might be even greater than it would be for an attached 'flat-plate' boundary layer with the same external-flow conditions that prevail outside the separated region. This conclusion was reached by considering the shear-layer flow between the separated region and the external stream. The shear layer was assumed to be at constant pressure everywhere except close to reattachment and to be a long way from the wall over most of its length, so that the air between it and the wall could be considered to be virtually motionless. Chapman also assumed the temperature of this dead air to be the same as that of the wall. Then the shear layer would be like the mixing zone at the edge of a jet emerging into still air. If the boundary layer on the surface just upstream of the separated region were very thin, a theoretical solution could be found for laminar flow for any free-stream Mach number. For turbulent flow with a thin upstream boundary layer, Chapman considered only the incompressible case, using Tollmien's results[67] for the characteristics of the mixing layer. There is one streamline of constant velocity in this layer which divides air which has originated in the main stream from air which has been entrained from the dead-air region. Consider the flux of total energy on the dead-air side of the dividing streamline near the downstream end of the separated region. The dividing streamline meets the wall at the reattachment point, and the fluid inside is reversed and returns to the dead-air region, carrying its total energy with it. As it flows along the wall the reversed flow is assumed to slow down to a low velocity, and to take up the wall temperature before being entrained again by the mixing region. The difference between the energy flux returned to the dead-air region and the energy flux entrained must balance the average heat transfer at the wall over the length of the separated region. Chapman thus found that for incompressible turbulent flow the average heat transfer would be 6·3 times as great as for an attached 'flat-plate' boundary layer with the same external-flow conditions as prevail outside the separated shear layer.

This predicted high rate of heat transfer is surprising, because it is difficult to see how the postulated slow-moving reversed flow, which must form an inner reversed boundary layer on the wall, can possibly support a high rate of heat transfer. It might well be, however, that most of the heat transfer would occur close to reattachment, where the reversed boundary layer would be thin. It may be significant here that the highest values of h in separated regions in our experiments occurred at the downstream ends of the regions, as can be seen from Fig. 12. Also it is possible that Chapman overestimates the heat transfer by assuming that the air returned near reattachment to the dead-air region takes up the same temperature as the wall before being entrained again. This would be reasonable if the analysis predicted small rates of heat transfer, but if the heat transfer is large, one would perhaps expect the core of the dead-air region to be at some temperature intermediate between the wall temperature and the total temperature of the main stream. Then the entrained air would be at this intermediate temperature, and the heat transfer would be somewhat lower than Chapman's estimate.

Chapman states that for compressible turbulent flow the heat transfer would be less than his estimate for incompressible flow. The reduction would partly be due to the fact that turbulent mixing layers spread less rapidly in supersonic than in low-speed flow (*cf.* Ref. 28). However, with regard to this point it is interesting to note that the region of high shear behind the rear step in the present experiment spreads at least as rapidly as an incompressible mixing layer, as can be seen from Fig. 13. Conditions are of course not the same as for the type of mixing layer considered by Chapman, since there is a thick boundary layer upstream of the base. The expansion at the corner of the base accelerates this boundary-layer flow, so that it forms a region of gentle shear outside the high-shear region, whose development it must effect. Because of these considerations, and because the separated regions are not large enough to make the pressure constant over the major part of their length, as assumed by Chapman, direct comparison with Chapman's results is not possible. Nevertheless, his theory does give an indication of how high rates of heat transfer may occur in separated regions, though, as discussed in the previous paragraph, the role of the reversed flow near the surface is not made clear.

Naysmith[47], who has done experiments on a reattaching flow behind a step, has suggested that the high rates of heat transfer downstream of reattachment can be interpreted as due to a thin 'inner boundary layer' starting from the reattachment position. His Mach-number profiles suggest this interpretation more forcibly than the profiles of Fig. 13 do, since Naysmith's profiles close to reattachment show flat regions near the wall, as though the edge of the boundary layer were close to the wall. The profiles of Fig. 13 have points of inflection, but these are not so marked as in Naysmith's experiments, perhaps because he was working with a much thinner boundary layer upstream of the base. However, profiles similar to our results of Fig. 13 have been obtained in various low-speed investigations of reattaching flows, cited by Coles in his paper[17] on 'the law of the wake'. Coles suggests that any turbulent boundary-layer profile can be regarded as a linear combination of a wake-like component and a component satisfying the 'law of the wall'. Equivalent to this would be a combination of a component of the shape of a flat-plate boundary-layer profile with a component of the shape of the profile at a separation or reattachment point. The flat-plate component would have an effective external velocity of zero at reattachment, but this would increase downstream. The thickness of the flat-plate component would be the total thickness of the real boundary layer, so in this respect Cole's interpretation would differ from Naysmith's. However, the effective external velocity, either for the flat-plate component or for the inner boundary layer, would probably, for a considerable distance downstream of reattachment, remain less than the external velocity would be if the step were removed and the flow remained attached everywhere. This suggests that the ratio of h to τ_w just downstream of reattachment would be greater than with the step removed, since where conditions are equivalent to the flow over a flat plate with external velocity u_1,

$$\frac{h}{\tau_w} = \frac{2C_p St}{u_1 C_f} \simeq \frac{1 \cdot 2 C_p}{u_1} .$$

Of course the heat transfer is by no means zero at a reattachment point, so the separation-profile or reattachment-profile component would have an effect as regards heat transfer, but still these considerations do perhaps throw light on why h in Fig. 12 behind the downstream reattachment point should be greater than its value in the absence of a step, whilst τ_w is considerably less.

The high heat-transfer rates found just in front of the forward step may be explained similarly. Here the skin friction τ_w is not particularly small, so it seems reasonable that h should be large. The concept of an effective inner boundary layer seems more definite here because of the reversed flow, and at any given distance from the step the maximum reversed velocity in the middle of the so-called dead-air region can be regarded as the effective external velocity for the inner boundary layer at the wall. The local maximum of h just upstream of separation may be associated with the rise of pressure at this position.

Thus, although the results of Fig. 12 for the heat transfer cannot be completely explained, they seem quite sensible viewed in the light of the considerations outlined above, taken in conjunction with Chapman's demonstration that the average heat transfer may be large in separated regions.

It remains to discuss the results for the effective recovery factor r_e. This was calculated from equation (23) with $M_1 = 2 \cdot 44$. The values could not be reliably estimated close to the rear step because h was small there, so that T_{re} could not be found accurately from equation (20). As pointed out earlier, where r_e varies from point to point it is not necessarily the same as the recovery factor would be for an insulated wall. However, it might be expected to vary in a roughly similar way. Brinich's results[10] and those of Bernstein and Brunk[3] for recovery factor resemble those of Fig. 12, though they do not indicate such a big increase of recovery factor just upstream of a step. Downstream of the rear step the data of Fig. 12 show a trough in the values for r_e, and this agrees with Brinich's findings. However, his results for heat transfer do not agree with Fig. 12, since he found Stanton numbers behind roughness elements slightly less than they would be with the elements removed. The cause of this discrepancy is not known.

8. *Conclusions and Summary.* Measurements have been made of heat transfer, skin friction, and boundary-layer profiles, in a turbulent boundary layer with a free-stream Mach number of $2 \cdot 44$. Results were obtained for a flat surface and for separated regions formed by forward-facing and rearward-facing steps. A steady-state method was used for the heat-transfer measurements, the surface being heated electrically and the power dissipated in an element of the surface being measured. Surface tubes of different heights were used to measure skin friction. The use of these types of heat-transfer and skin-friction instruments in supersonic flow is discussed in Sections 4 and 5. For the flat surface the results for heat transfer agreed approximately with the findings of other workers, but the skin-friction results were higher than accepted values, due probably to compressibility effects on the Stanton tubes. It would appear that such compressibility effects are not linear in the tube height, since the results given by the different tubes showed little consistent trend with tube height. In the separated region ahead of a forward-facing step, high rates of heat transfer were measured close to the step, and the heat transfer was also quite high downstream of reattachment behind a rearward-facing step. A physical explanation which partially accounts for these findings is advanced in Section 7, and is based on a consideration of an effective inner boundary layer, taking into account Chapman's theoretical analysis for heat transfer in separated regions.

Acknowledgements. The authors were greatly assisted in formulating their ideas by discussions with Mr. P. Bradshaw and Dr. I. Hall of N.P.L. and with Mr. A. Naysmith of R.A.E.

The apparatus, which presented considerable difficulties of design and manufacture, was designed by Mr. C. Culverhouse and made by Mr. J. D. Darcy.

LIST OF SYMBOLS

C_f	Coefficient of local skin friction $2\tau_w/\rho_1 u_1^2$
C_{fi}	C_f for related 'flat-plate' incompressible boundary layer (*cf.* equation (1))
C_F	Coefficient of average skin friction $\frac{1}{x_e}\int_0^{x_e} C_f\, dx_e = \frac{2\theta}{x_e}$
C_{Fi}	C_F for related 'flat-plate' incompressible boundary layer (*cf.* equation (1))
C_p	Specific heat at constant pressure
d	Total height (opening plus lip thickness) of Stanton tube above surrounding surface
d'	Defines 'effective measurement position' for Stanton tube according to equation (6)
h	Rate of heat transfer per unit area divided by difference between wall temperature T_w (assumed uniform) and effective recovery temperature T_{re}
L	Term independent of wall temperature appearing in equation (22), associated largely with conduction between heat-transfer unit and surrounding liner
M	Mach number
M_1	M just outside boundary layer
p	Static pressure
Δp	Difference between Stanton-tube pressure and p
r	Recovery factor for insulated wall, $(T_{aw} - T_1)/(T_s - T_1)$, where T_{aw} is adiabatic wall temperature
r_e	Effective recovery factor for heat transfer from body with uniform surface temperature, equal to $(T_{re} - T_1)/(T_s - T_1)$ or given by equation (23)
R_θ	Reynolds number based on momentum thickness θ and conditions at edge of boundary layer
$R_{\theta i}$	R_θ for related 'flat-plate' incompressible boundary layer (*cf.* equation (1))
R_s	Stanton-tube Reynolds number defined by equation (7)
R_{xe}	Reynolds number based on distance x_e from 'effective leading edge' and conditions at edge of boundary layer
St	Stanton number $h/\rho_1 C_p u_1$
St_i	St for related 'flat-plate' incompressible boundary layer (*cf.* equation (1))
$\overline{St}$	Average Stanton number $\frac{1}{x_e}\int_0^{x_e} St\, dx_e$
$\overline{St}_i$	$\overline{St}$ for related 'flat-plate' incompressible boundary layer (*cf.* equation (1))
t	Thickness of laminar sublayer
T_{av}	Average of temperatures recorded by the four thermo-couples in supporting disc of heat-transfer unit
T_{0av}	T_{av} with no heating currents applied
T_{th}	Temperature recorded by thermo-couple in top of thimble of heat-transfer unit
T_{0th}	T_{th} with no heating currents applied
T_1	Temperature at edge of boundary layer, in deg K
T_w	Wall temperature in deg K

T_s	Stagnation temperature in deg K
T_{0s}	T_s with no heating currents applied
T_{re}	Effective recovery temperature, equal to the value of T_w which makes the heat transfer locally zero when T_w is uniform
u_1	Velocity at edge of boundary layer
W	Wattage to bulb of heat-transfer unit
x_e	Distance from effective leading edge of turbulent boundary layer
y	Distance from wall along normal
δ	Total thickness of boundary layer
θ	Momentum thickness of boundary layer
μ_w	Viscosity at wall
ρ_w	Density at wall
ρ_1	Density at edge of boundary layer
τ_w	Skin friction

REFERENCES

No.	Author	Title, etc.
1	S. S. Abarbanel, R. J. Hakkinen and L. Trilling	The use of Stanton tube for skin-friction measurements. Fluid Dynamics Research Group. Massachusetts Institute of Technology. Tech. Report 57–3. 1957.
2	J. J. Bernard and R. Siestrunck ..	Échanges de chaleur dans les écoulements présentant des décollements. Paper presented at the First International Congress of Aeronautical Sciences, Madrid. September, 1958.
3	H. Bernstein and W. E. Brunk ..	Exploratory investigation of flow in the separated region ahead of two blunt bodies at Mach number 2. N.A.C.A. Research Memo. E55D07b, TIB/4590. June, 1955.
4	H. L. Bloom	Preliminary survey of boundary-layer development at a nominal Mach number of 5·5. N.A.C.A. Research Memo. E52D03, TIB/3031. June, 1952.
5	W. S. Bradfield and D. G. DeCoursin	Measurements of turbulent heat transfer on bodies of revolution at supersonic speeds. *J. Ae. Sci.* 23. pp. 272 to 274. No. 3. March, 1956.
6	P. Bradshaw and N. Gregory	Calibration of Preston tubes on a flat plate using measurements of local skin friction. A.R.C. 20, 199. May, 1958.
7	M. J. Brevoort and B. D. Arabian ..	Summary of experimental heat-transfer measurements in turbulent flow for a Mach-number range from 0·87 to 5·05. N.A.C.A. Tech. Note 4248. May, 1958.
8	P. F. Brinich	Boundary-layer measurements in 3·84 by 10 in. supersonic channel. N.A.C.A. Tech. Note 2203. October, 1950.
9	P. F. Brinich and N. S. Diaconis ..	Boundary-layer development and skin friction at Mach number 3·05. N.A.C.A. Tech. Note 2742. July, 1952.
10	P. F. Brinich	Recovery temperatures and heat transfer near two-dimensional roughness elements at Mach 3·1. N.A.C.A. Tech. Note 4213. February, 1958.
11	D. R. Chapman and R. H. Kester ..	Measurements of turbulent skin friction on cylinders in axial flow at subsonic and supersonic velocities. *J. Ae. Sci.* 20. No. 7. pp. 441 to 448. July, 1953.
12	D. R. Chapman and R. M. Kester ..	Turbulent boundary-layer and skin-friction measurements in axial flow along cylinders at Mach numbers between 0·5 and 3·6. N.A.C.A. Tech. Note 3097. March, 1954.
13	D. R. Chapman..	A theoretical analysis of heat transfer in regions of separated flow. N.A.C.A. Tech. Note 3792. October, 1956.

No.	Author	Title, etc.
14	B. des Clers and J. Sternberg	On boundary-layer temperature recovery factors. *J. Ae. Sci.* 19. No. 9. pp. 645 to 646. September, 1952.
15	D. Coles	Measurements in the boundary layer on a smooth flat plate in supersonic flow. III—Measurements in a flat-plate boundary layer at the Jet Propulsion Laboratory. Jet Propulsion Laboratory, California Institute of Technology. Report 20–71. June, 1953.
16	D. Coles	Measurements of turbulent friction on a smooth flat plate in supersonic flow. *J. Ae. Sci.* 21. No. 7. pp. 433 to 448. July, 1954.
17	D. Coles	The law of the wake in the turbulent boundary layer. *J. Fluid Mech.* 1. Part 2. pp. 191 to 226. July, 1956.
18	W. F. Cope	The measurement of skin friction in a turbulent boundary layer at a Mach number of 2·5, including the effect of a shock wave. *Proc. Roy. Soc.* A. Vol. 215. 84. 1952.
19	W. F. Cope	Notes and graphs for boundary-layer calculations in compressible flow. C.P. 89. August, 1951.
20	W. F. Cope	The turbulent boundary layer in compressible flow. R. & M. 2840. November, 1943.
21	D. G. DeCoursin, W. S. Bradfield and J. J. Sheppard	Aerodynamic heating and heat-transfer phenomena at Mach numbers 2·7 through 5·7. Wright Air Development Center. W.A.D.C. Technical Report 53–379. 1954.
22	C. duP. Donaldson	On the form of the turbulent skin-friction law and its extension to compressible flows. N.A.C.A. Tech. Note 2692. May, 1952.
23	G. R. Eber	Recent investigation of temperature recovery and heat transmission on cones and cylinders in axial flow in the N.O.L. Aeroballistics Wind Tunnel. *J. Ae. Sci.* 19. No. 1. p. 1. January, 1952.
24	E. R. G. Eckert and J. N. B. Livingood	Method for calculation of laminar heat transfer in airflow around cylinders of arbitrary cross-section (including large temperature differences and transpiration cooling). N.A.C.A. Report 1118. 1953.
25	H. U. Eckert	Characteristics of the turbulent boundary layer on a flat plate in compressible flow from measurements of friction in pipes. *J. Ae. Sci.* 17. No. 9. pp. 573 to 584. September, 1950.
26	W. B. Fallis	Heat transfer in the transitional and turbulent boundary layers of a flat plate at supersonic speeds. Institute of Aerophysics, University of Toronto. U.T.I.A. Report 19. May, 1952.

No.	Author	Title, etc.
27	S. Goldstein (editor)	*Modern Developments in Fluid Dynamics*. Vol. II. p. 362. Oxford University Press. 1938.
28	P. B. Gooderum, G. P. Wood and M. J. Brevoort	Investigation with an interferometer of the turbulent mixing of a free supersonic jet. N.A.C.A. Report 963. 1950.
29	D. W. Holder and G. E. Gadd ..	The interaction between shock waves and boundary layers and its relation to base pressure in supersonic flow. Paper No. 8 of 'Boundary-Layer Effects in Aerodynamics'; proceedings of a Symposium held at the N.P.L. on 31st March and 1st April, 1955. H.M.S.O. 1955.
30	J. N. Hool	Measurement of skin friction using surface tubes. *Air. Eng.* 28. 52. 1956.
31	J. R. Jack and N. S. Diaconis	Heat-transfer measurements on two bodies of revolution at a Mach number of 3·12. N.A.C.A. Tech. Note 3776. October, 1956.
32	J. Kaye	Survey of friction coefficients, recovery factors, and heat-transfer coefficients for supersonic flow. *J. Ae. Sci.* 21. No. 2. pp. 117 to 129. February, 1954.
33	C. E. Kepler and S. M. Bogdonoff ..	Interaction of a turbulent boundary layer with a step at $M = 3$. Princeton University, Department of Aeronautical Engineering. Report 238. September, 1953.
34	R. H. Korkegi	Transition studies and skin-friction measurements on an insulated flat plate at a Mach number of 5·8. *J. Ae. Sci.* 23. No. 2. pp. 97 to 107 and 192. February, 1956
35	I. Korobkin	On the determination of local heat-transfer coefficients for bodies with pressure gradient in supersonic flow. *J. Ae. Sci.* 22. No. 4. p. 283. April, 1955.
36	H. H. Kurzweg	The status of heat transfer and friction investigations at supersonic speeds. AGARD papers presented at the seventh meeting of the Wind Tunnel and Model Testing Panel. AG 19/P9. pp. 207 to 215. Canada. June, 1955.
37	H. W. Liepmann and G. T. Skinner ..	Shearing-stress measurements by use of a heated element. N.A.C.A. Tech. Note 3268. November, 1954.
38	R. K. Lobb, E. M. Winkler and J. Persh	Experimental investigation of turbulent boundary layers in hypersonic flow. *J. Ae. Sci.* 22. No. 1. pp. 1 to 9 and 50. January, 1955.
39	H. Ludwieg	Ein Gerät zur Messung der Wandschubspannung turbulenter Reibungsschichten. *Ing.-Arch.* 17. No. 3. pp. 207 to 218. 1949. Translated as: Instrument for measuring the wall-shearing stress of turbulent boundary layers. N.A.C.A. Tech. Memo. 1284. May, 1950.

No.	*Author*	*Title, etc.*
40	L. M. Mack	Summary of existing cone temperature recovery factor data obtained in continuous-flow wind tunnels plus additional data. *J. Ae. Sci.* 22. No. 3. pp. 212 to 214. March, 1955.
41	R. J. Monaghan	Comparison between experimental measurements and a suggested formula for the variation of turbulent skin friction in compressible flow. C.P. 45. February, 1950.
42	R. J. Monaghan and J. E. Johnson ..	The measurement of heat transfer and skin friction at supersonic speeds. Preliminary results of measurements on a flat plate at a Mach number of 2·5. C.P. 59. April, 1949.
43	R. J. Monaghan and J. E. Johnson ..	The measurement of heat transfer and skin friction at supersonic speeds. Part II—Boundary-layer measurements on a flat plate at $M = 2 \cdot 5$ and zero heat transfer. C.P. 64. December, 1949.
44	R. J. Monaghan and J. R. Cooke ..	The measurement of heat transfer and skin friction at supersonic speeds. Part III—Measurements of overall heat transfer and of the associated boundary layers on a flat plate at $M = 2 \cdot 43$. C.P. 139. December, 1951.
45	R. J. Monaghan and J. R. Cooke ..	The measurement of heat transfer and skin friction at supersonic speeds. Part IV—Tests on a flat plate at $M = 2 \cdot 82$. C.P. 140. June, 1952.
46	R. J. Monaghan	A review and assessment of various formulae for turbulent skin friction in compressible flow. C.P. 142. August, 1952.
47	A. Naysmith	Heat-transfer and boundary-layer measurements in a region of supersonic flow separation and reattachment. A.R.C. 20, 601. May, 1958.
48	R. M. O'Donnell	Experimental investigation at a Mach number of 2·41 of average skin-friction coefficients and velocity profiles for laminar and turbulent boundary layers and an assessment of probe effects. N.A.C.A. Tech. Note 3122. January, 1954.
49	C. C. Pappas	Measurement of heat transfer in the turbulent boundary layer on a flat plate in supersonic flow and comparison with skin-friction results. N.A.C.A. Tech. Note 3222. January, 1954.
50	J. H. Preston	The determination of turbulent skin friction by means of pitot tubes. *J. R. Ae. Soc.* 58. No. 518. pp. 109 to 121, February, 1954.
51	E. F. Relf, R. C. Pankhurst and W. S. Walker	The use of pitot-tubes to measure skin friction on a flat plate. A.R.C. 17, 025. August, 1954.

No.	Author	Title, etc.
52	D. Ross	Evaluation of the momentum integral equation for turbulent boundary layers. *J. Ae. Sci.* 20. No. 7. p. 502. July, 1953.
53	M. W. Rubesin, R. C. Maydew and S. A. Varga	An analytical and experimental investigation of the skin friction of the turbulent boundary layer on a flat plate at supersonic speeds. N.A.C.A. Tech. Note 2305. February, 1951.
54	M. W. Rubesin	The effect of an arbitrary surface-temperature variation along a flat plate on the convective heat transfer in an incompressible turbulent boundary layer. N.A.C.A. Tech. Note 2345. April, 1951.
55	M. W. Rubesin, C. B. Rumsey and S. A. Varga	A summary of available knowledge concerning skin friction and heat transfer and its application to the design of high-speed missiles. N.A.C.A. Research Memo. A51J25a, TIB/2928. November, 1951.
56	L. F. Ryan	Experiments on aerodynamic cooling. Thesis presented to the Swiss Federal Institute of Technology, Zürich, for the degree of Doctor of Technical Science. Prom. No. 1981. 1951.
57	A. Seiff	Examination of the existing data on the heat transfer of turbulent boundary layers at supersonic speeds from the point of view of Reynolds analogy. N.A.C.A. Tech. Note 3284. August, 1954.
58	R. H. Shoulberg *et al.*	An experimental investigation of flat-plate heat-transfer coefficients at Mach numbers of 2, 2·5, and 3 for a surface temperature to stream total temperature ratio of 1·18. Massachusetts Institute of Technology. Naval Supersonic Laboratory Wind Tunnel Report 39. June, 1953.
59	R. H. Shoulberg, J. A. F. Hill and M. A. Rivas, Jr.	An experimental determination of flat-plate recovery factors for Mach numbers between 1·90 and 3·14. *J. Ae. Sci.* 21. No. 11. pp. 763 to 771. November, 1954.
60	E. G. Slack	Experimental investigation of heat transfer through laminar and turbulent boundary layers on a cooled flat plate at a Mach number of 2·4. N.A.C.A. Tech. Note 2686. April, 1952.
61	S. C. Sommer and B. J. Short ..	Free-flight measurements of turbulent-boundary-layer skin friction in the presence of severe aerodynamic heating at Mach numbers from 2·8 to 7·0. N.A.C.A. Tech. Note 3391. March, 1955.
62	J. R. Stalder, M. W. Rubesin and T. Tendeland	A determination of the laminar-, transitional-, and turbulent-boundary-layer temperature-recovery factors on a flat plate in supersonic flow. N.A.C.A. Tech. Note 2077. June, 1950.

No.	Author	Title, etc.
63	T. E. Stanton, D. Marshall and L. Bryant	On the conditions at the boundary of a fluid in turbulent motion. *Proc. Roy. Soc.* A. 97. 422. 1920.
64	H. A. Stine and R. Scherrer	Experimental investigation of the turbulent-boundary-layer temperature-recovery factor on bodies of revolution at Mach numbers from 2·0 to 3·8. N.A.C.A. Tech. Note 2664. March, 1952.
65	G. I. Taylor	Measurements with a half-pitot tube. *Proc. Roy. Soc.* A. 166. 476. 1938.
66	T. Tendeland	Effects of Mach number and wall-temperature ratio on turbulent heat transfer at Mach numbers from 3 to 5. N.A.C.A. Tech. Note 4236. April, 1958.
67	W. Tollmien	Berechnung turbulenter Ausbreitungsvorgänge. *Z.A.M.M.* 6. Part 6. pp. 468 to 478. December, 1926.
68	M. Tucker	Approximate turbulent boundary-layer development in plane compressible flow along thermally insulated surfaces with application to supersonic-tunnel contour correction. N.A.C.A. Tech. Note 2045. March, 1950.
69	E. R. Van Driest	Turbulent boundary layer in compressible fluids. *J. Ae. Sci.* 18. No. 3. pp. 145 to 160 and 216. March, 1951.
70	R. E. Wilson	Turbulent boundary-layer characteristics at supersonic speeds—theory and experiment. *J. Ae. Sci.* 17. No. 9. pp. 585 to 594. September, 1950.
71	W. R. Wimbrow	Experimental investigation of temperature recovery factors on bodies of revolution at supersonic speeds. N.A.C.A. Tech. Note 1975. October, 1949.

TABLE 1

Results for the Flat Surface

Run number	H_0 (in. Hg)	Front measurement station									Rear measurement station									
		M_1 (average)	$St.\ 10^3$	r_e	$C_f.\ 10^3$, unheated			$C_f.\ 10^3$, heated			M_1 (average)	$St.\ 10^3$	r_e	$C_f.\ 10^3$, unheated			$C_f.\ 10^3$, heated		
					A	B	C	A	B	C				A	B	C	A	B	C
1	30	2·46	1·21	0·874							2·44								
4	30	2·45	1·12	0·875							2·44								
6	30	2·43									2·43			2·29	2·24	2·28	2·35	2·19	2·19
7	30	2·43	1·04	0·870							2·44			2·39	2·16	2·25	2·44	2·13	2·28
10	30	2·44			2·48	2·44	2·48	2·48	2·42	2·48	2·43	1·03	0·879						
13	30	2·45	1·02	0·867							2·44			2·47	2·25	2·29	2·38	2·23	2·28
3	20	2·45	1·24	0·871							2·43								
9	20	2·44	1·10	{0·855 0·866}							2·44			{2·56 2·55 2·59	2·32 2·22 2·26	2·41 2·43 2·32	2·71 2·71 2·63	2·36 2·34 2·26	2·42 2·36 2·28
11	20	2·42			2·80	2·60	2·60	2·84	2·70	2·65	2·44	1·05	0·874						
2	13	2·42	1·30	0·873							2·42								
5	13	2·41	1·19	0·880							2·41								
8	13	2·43	1·17	0·873							2·43			2·83	2·50	2·48	2·73	2·82	2·52
12	13	2·42			2·98	2·92	2·78	3·13	3·02	2·85	2·42	1·14	0·905						

TABLE 2

Boundary-Layer Characteristics for the Unheated Flat Surface

H_0 (in. Hg)	Front measurement station			Rear measurement station		
	θ (in.)	δ (in.)	θ/δ	θ (in.)	δ (in.)	θ/δ
30	0·0300	0·380	0·0789	0·0495	0·640	0·0774
20	0·0313	0·415	0·0754	0·0526	0·690	0·0762
13	0·0331	0·445	0·0745	0·0562	0·730	0·0770

TABLE 3

Comparison with Incompressible Results

H_0 (in. Hg)	Front measurement station					Rear measurement station				
	R_θ	Mean $C_f \cdot 10^3$	C_f/C_{fi}	Mean $St. 10^3$	St/St_i	R_θ	Mean $C_f \cdot 10^3$	C_f/C_{fi}	Mean $St. 10^3$	St/St_i
30	7500	2·47	0·907	1·10	0·716	12390	2·29	0·945	1·03	0·754
20	5220	2·67	0·901	1·17	0·701	8770	2·41	0·919	1·05	0·712
13	3580	2·89	0·890	1·22	0·674	6100	2·60	0·910	1·14	0·707

TABLE 4

Watts W to Heat-Transfer Unit Bulb in Separated Regions when the Thimble Temperature T_{th} is equal to the Surrounding Temperature T_{av}

Forward-facing step				Rearward-facing step			
Distance from step (in.)	T_{av} (deg C)	T_s (deg C)	W	Distance from step (in.)	T_{av} (deg C)	T_s (deg C)	W
0·78	65·8	43·4	1·72	0·46	64·6	40·2	−0·13
1·78	62·8	41·3	1·17	0·96	67·6	41·2	+0·21
2·78	68·0	41·9	1·29	1·46	65·2	38·6	1·19
3·78	65·2	41·0	1·63	2·46	57·6	38·8	1·86
4·78	64·5	40·9	1·91	3·46	63·0	37·9	2·52
5·78	66·0	42·2	1·51	4·46	62·8	38·5	2·43
6·78	68·2	43·4	1·55	5·46	59·2	38·1	2·35
				6·46	62·5	40·1	+2·28

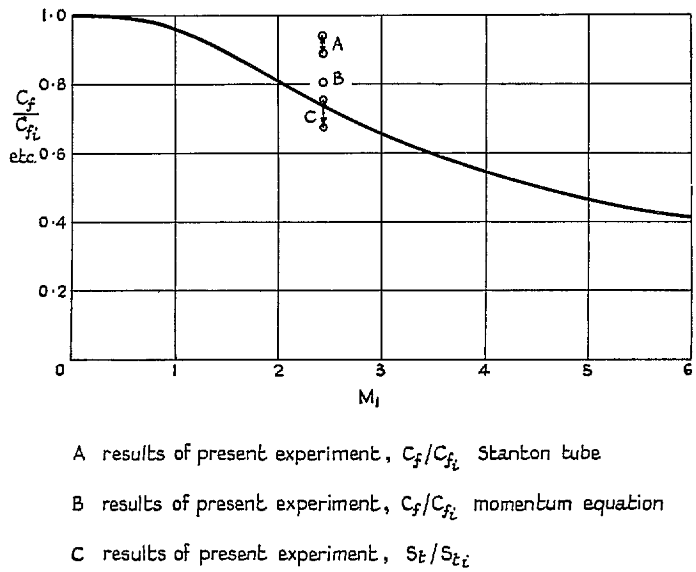

FIG. 1. Mean curve for C_f/C_{fi}, C_F/C_{Fi}, St/St_i, or $\overline{St}/\overline{St}_i$ as a function of free-stream Mach number M_1; 'flat-plate' results.

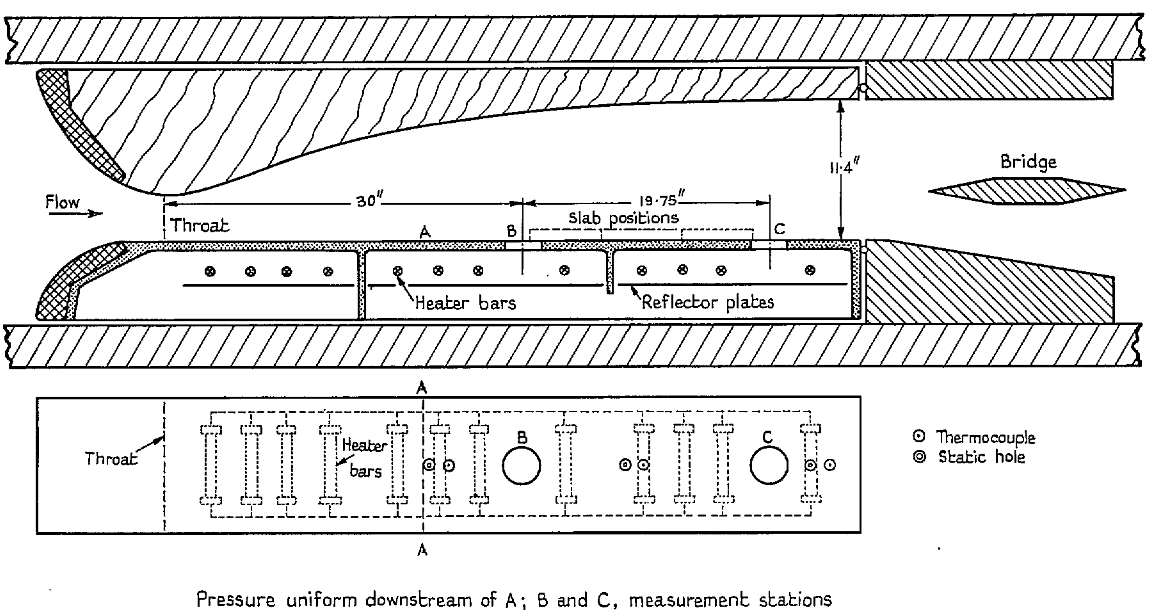

FIG. 2. The arrangement of the working-section and plan of the test liner.

(78647) C

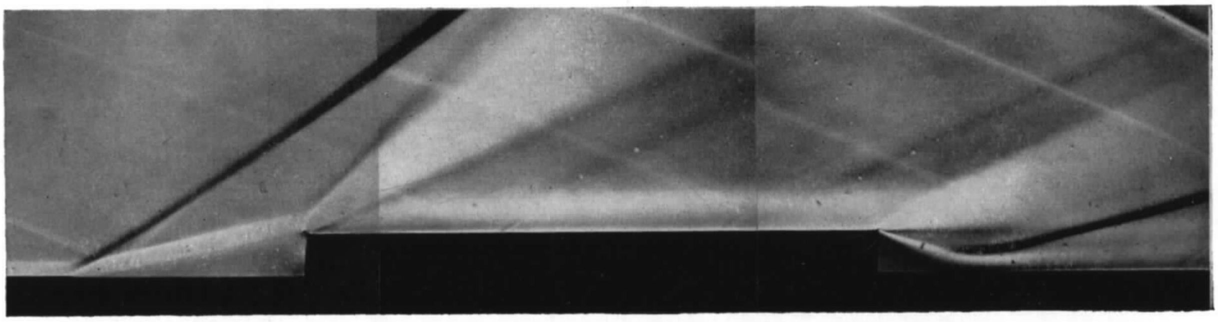

FIG. 3. Composite schlieren picture of the flow over the slab.

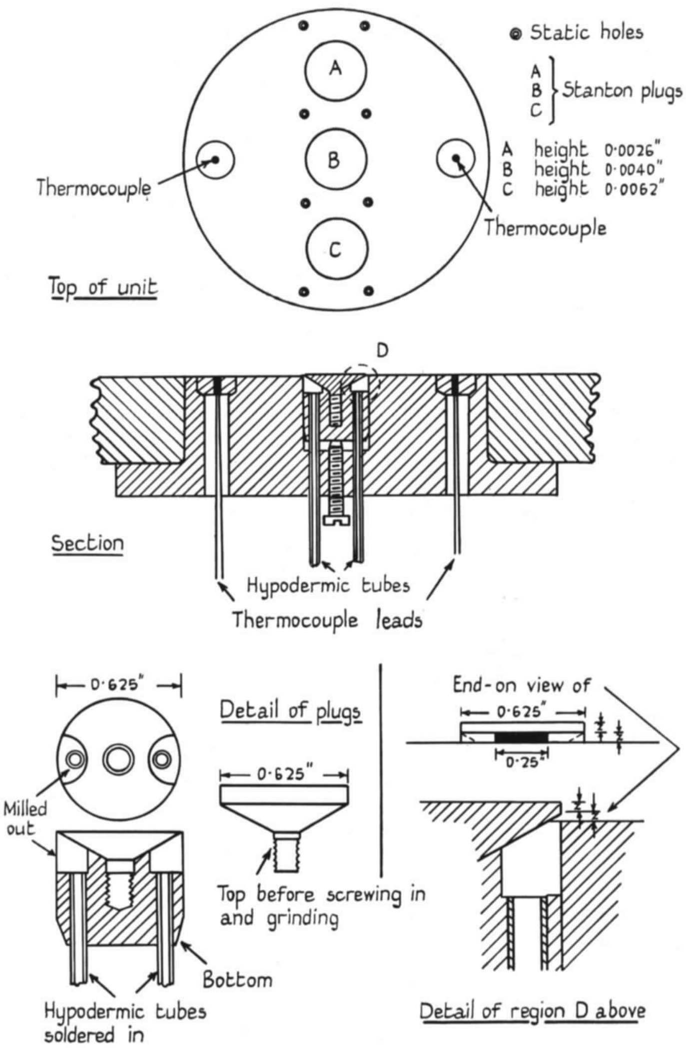

FIG. 4. Stanton-tube unit.

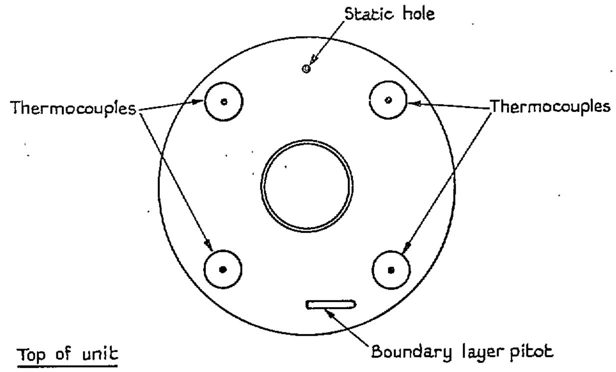

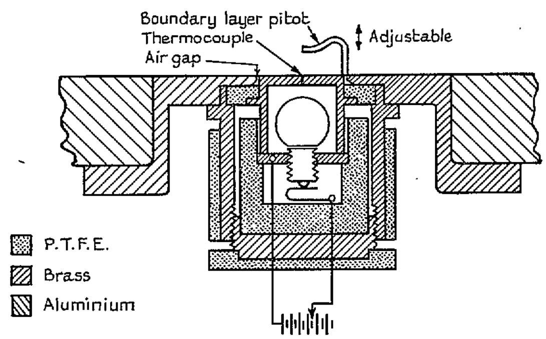

FIG. 5. Heat-transfer unit.

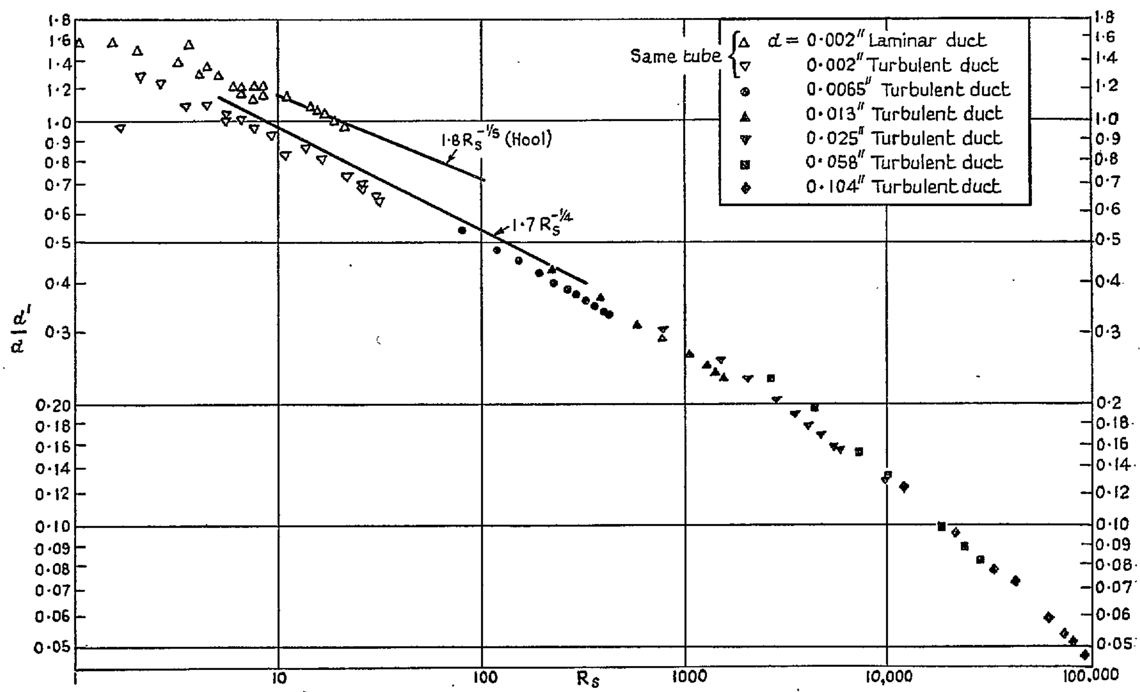

FIG. 6. Bradshaw's Stanton-tube calibration results.

(78647) C*

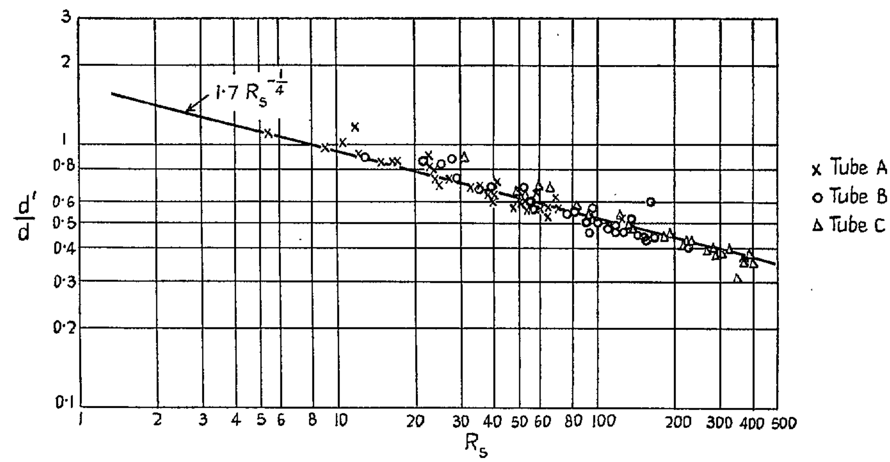

FIG. 7. Stanton-tube calibration results for forward and rearward facing tubes before and after main experiments.

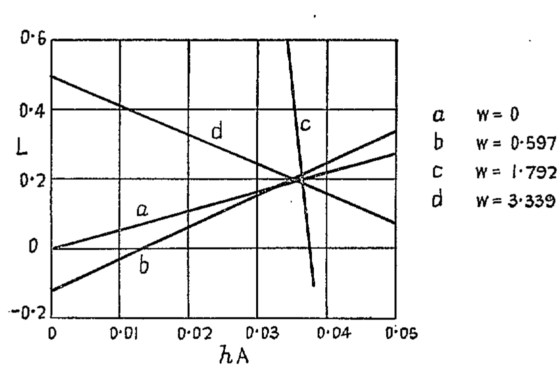

FIG. 8. Intersections for rear measurement station, flat surface, $H_0 = 30$ in. Hg. Estimated intersection: $L = 0 \cdot 20$, $hA = 0 \cdot 0355$ Watts deg C.

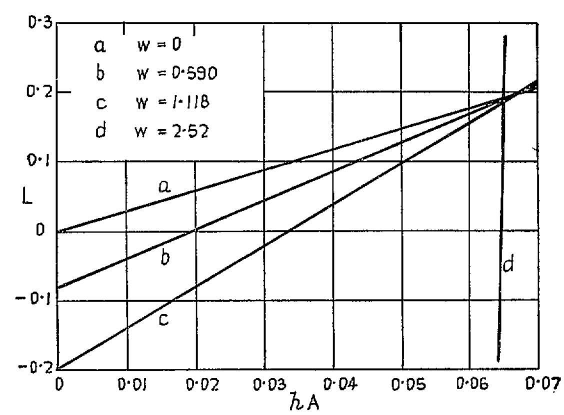

FIG. 9. Intersections for unit in separated region, 0·78 in. upstream of forward-facing step. Estimated intersection: $L = 0 \cdot 185$, $hA = 0 \cdot 0655$ Watts deg C.

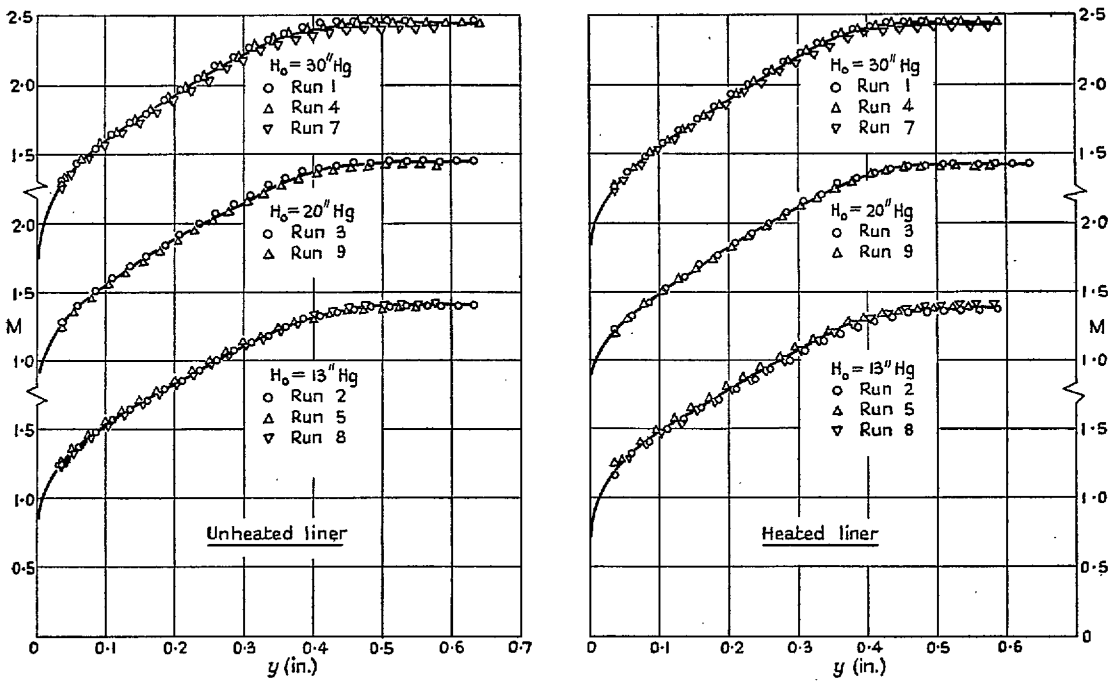

FIG. 10. Boundary-layer profiles for flat surface at forward measurement position.

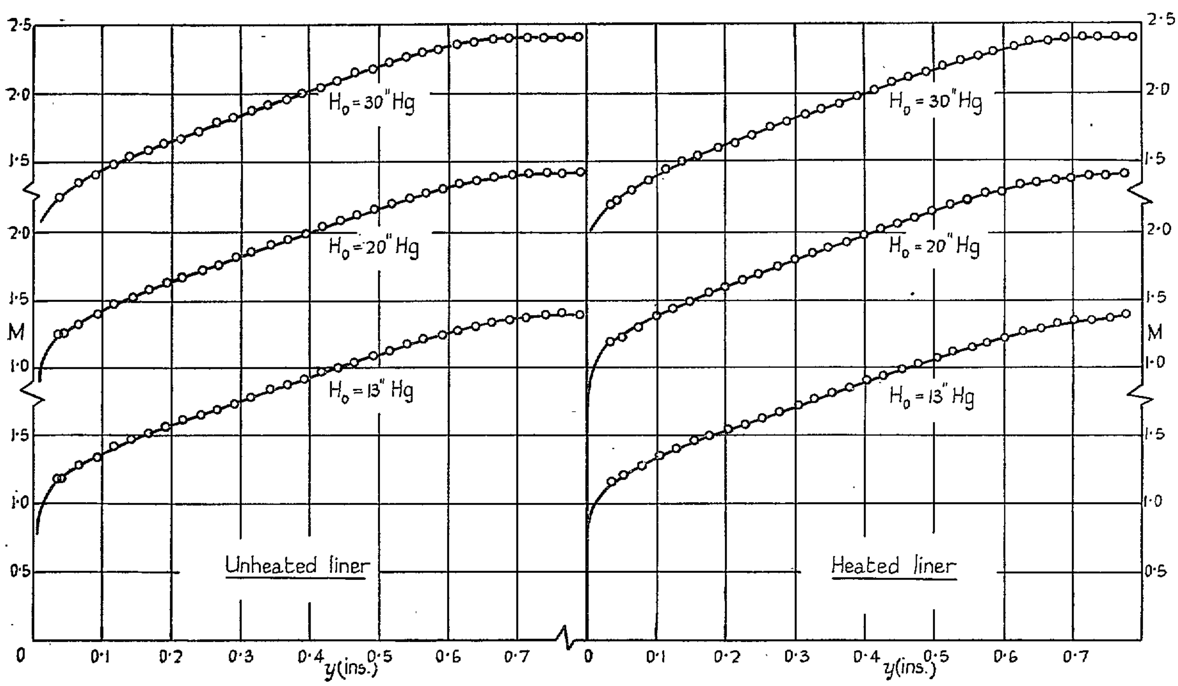

FIG. 11. Boundary-layer profiles for flat surface at rear measurement station.

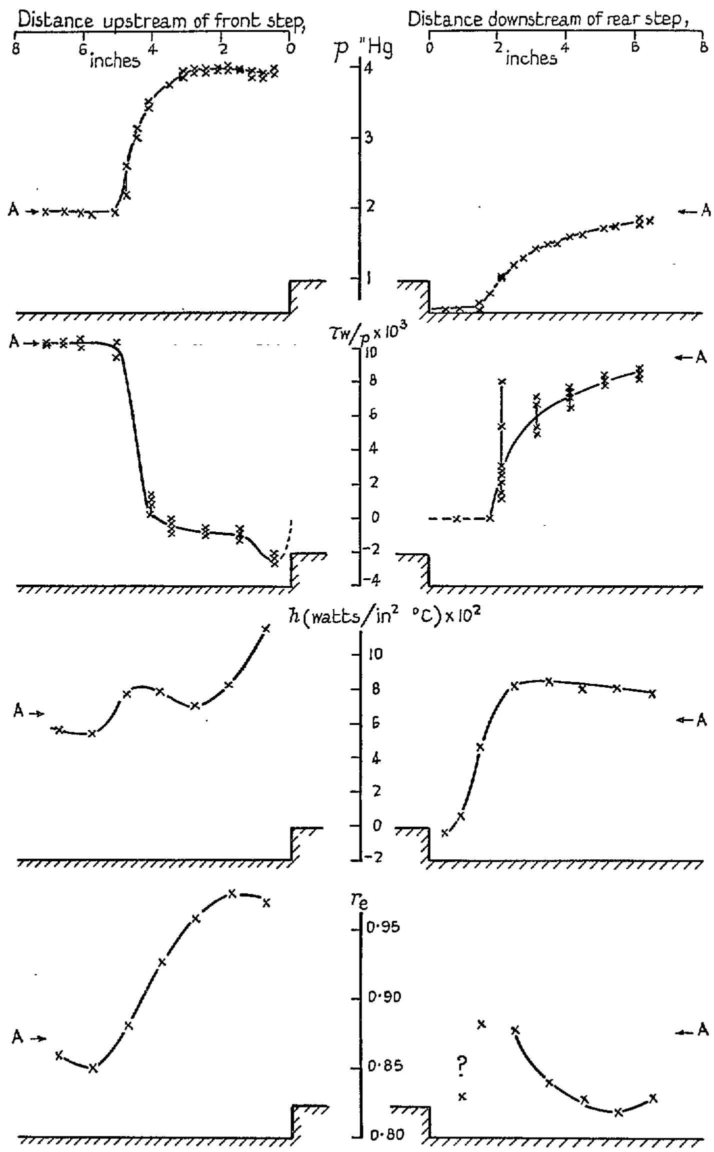

FIG. 12. Results for the separated regions. 'A' denotes average 'no-step' values.

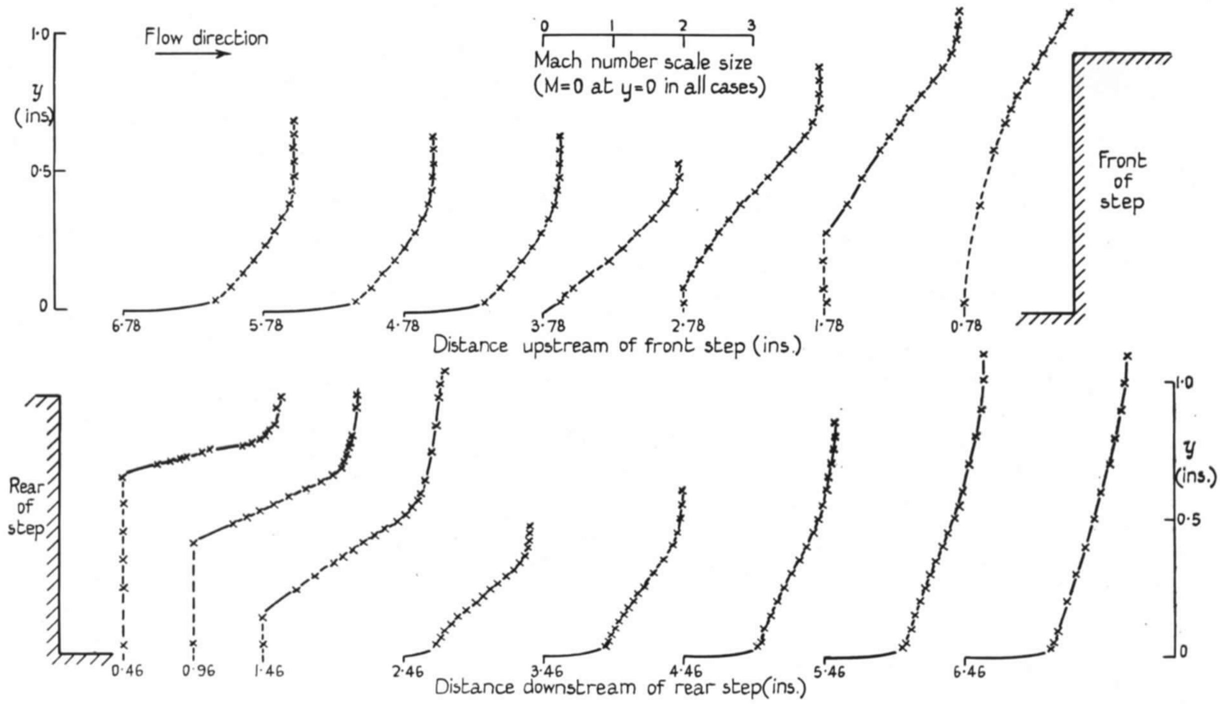

FIG. 13. Mach-number profiles through the separated regions.

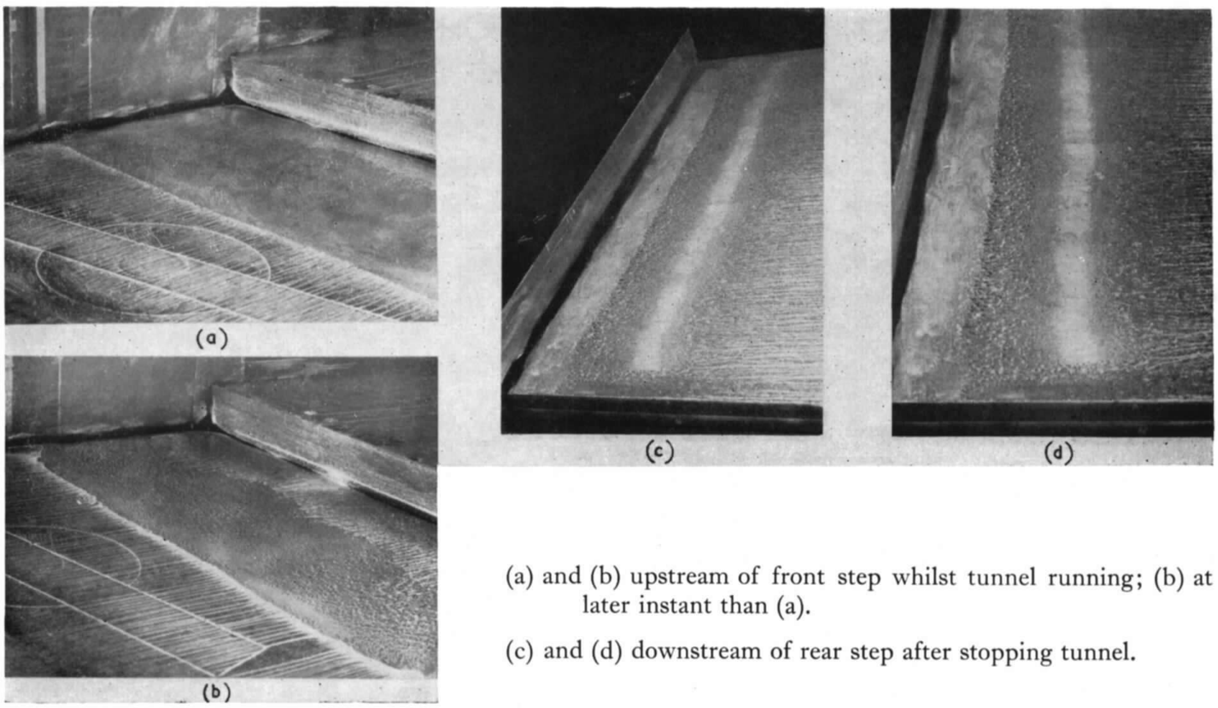

(a) and (b) upstream of front step whilst tunnel running; (b) at later instant than (a).

(c) and (d) downstream of rear step after stopping tunnel.

FIGS. 14a to 14d. Oil-flow patterns showing the flow at the surface.

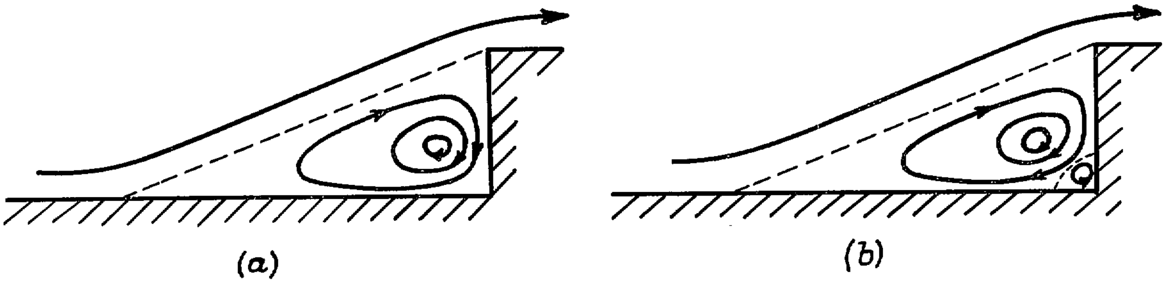

FIG. 15. Possible streamline patterns upstream of a forward-facing step.

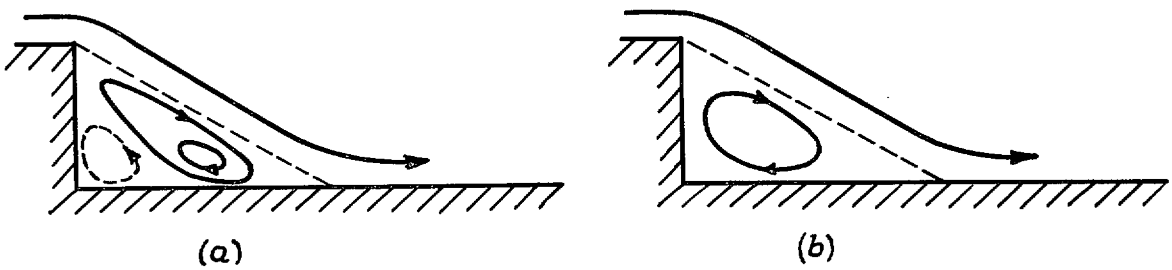

FIG. 16. Possible streamline patterns downstream of rearward-facing step.

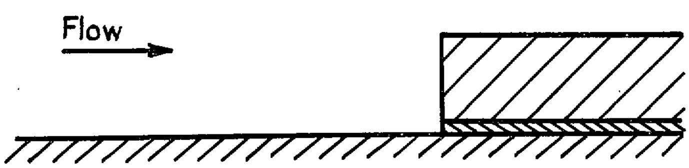

FIG. 17. Hypothetical layer of thermal insulator between the step and the liner.

(78647) Wt. 54/8210 K.5 9/60 Hw.

Publications of the Aeronautical Research Council

ANNUAL TECHNICAL REPORTS OF THE AERONAUTICAL RESEARCH COUNCIL (BOUND VOLUMES)

1941 Aero and Hydrodynamics, Aerofoils, Airscrews, Engines, Flutter, Stability and Control, Structures. 63*s*. (post 2*s*. 3*d*.)

1942 Vol. I. Aero and Hydrodynamics, Aerofoils, Airscrews, Engines. 75*s*. (post 2*s*. 3*d*.)
Vol. II. Noise, Parachutes, Stability and Control, Structures, Vibration, Wind Tunnels. 47*s*. 6*d*. (post 1*s*. 9*d*.)

1943 Vol. I. Aerodynamics, Aerofoils, Airscrews. 80*s*. (post 2*s*.)
Vol. II. Engines, Flutter, Materials, Parachutes, Performance, Stability and Control, Structures. 90*s*. (post 2*s*. 3*d*.)

1944 Vol. I. Aero and Hydrodynamics, Aerofoils, Aircraft, Airscrews, Controls. 84*s*. (post 2*s*. 6*d*.)
Vol. II. Flutter and Vibration, Materials, Miscellaneous, Navigation, Parachutes, Performance, Plates and Panels, Stability, Structures, Test Equipment, Wind Tunnels. 84*s*. (post 2*s*. 6*d*.)

1945 Vol. I. Aero and Hydrodynamics, Aerofoils. 130*s*. (post 2*s*. 9*d*.)
Vol. II. Aircraft, Airscrews, Controls. 130*s*. (post 2*s*. 9*d*.)
Vol. III. Flutter and Vibration, Instruments, Miscellaneous, Parachutes, Plates and Panels, Propulsion. 130*s*. (post 2*s*. 6*d*.)
Vol. IV. Stability, Structures, Wind Tunnels, Wind Tunnel Technique. 130*s*. (post 2*s*. 6*d*.)

Special Volumes

Vol. I. Aero and Hydrodynamics, Aerofoils, Controls, Flutter, Kites, Parachutes, Performance, Propulsion, Stability. 126*s*. (post 2*s*. 6*d*.)
Vol. II. Aero and Hydrodynamics, Aerofoils, Airscrews, Controls, Flutter, Materials, Miscellaneous, Parachutes, Propulsion, Stability, Structures. 147*s*. (post 2*s*. 6*d*.)
Vol. III. Aero and Hydrodynamics, Aerofoils, Airscrews, Controls, Flutter, Kites, Miscellaneous, Parachutes, Propulsion, Seaplanes, Stability, Structures, Test Equipment. 189*s*. (post 3*s*. 3*d*.)

Reviews of the Aeronautical Research Council

1939–48 3*s*. (post 5*d*.) 1949–54 5*s*. (post 6*d*.)

Index to all Reports and Memoranda published in the Annual Technical Reports

1909–1947 R. & M. 2600 6*s*. (post 4*d*.)

Author Index to the Reports and Memoranda and Current Papers of the Aeronautical Research Council

February, 1954–February, 1958 R & M. No. 2570 (Revised) (Addendum) 7*s*. 6*d*. (post 4*d*.)

Indexes to the Technical Reports of the Aeronautical Research Council

July 1, 1946–December 31, 1946 R. & M. No. 2150 1*s*. 3*d*. (post 2*d*.)

Published Reports and Memoranda of the Aeronautical Research Council

Between Nos. 2251–2349	R. & M. No. 2350	1*s*. 9*d*. (post 2d.)
Between Nos. 2351–2449	R. & M. No. 2450	2*s*. (post 2*d*.)
Between Nos. 2451–2549	R. & M. No. 2550	2*s*. 6*d*. (post 2*d*.)
Between Nos. 2551–2649	R. & M. No. 2650	2*s*. 6*d*. (post 2*d*.)
Between Nos. 2651–2749	R. & M. No. 2750	2*s*. 6*d*. (post 2*d*.)
Between Nos. 2751–2849	R. & M. No. 2850	2*s*. 6*d*. (post 2*d*.)
Between Nos. 2851–2949	R. & M. No. 2950	3*s*. (post 2*d*.)

HER MAJESTY'S STATIONERY OFFICE

from the addresses overleaf

Printed and published by
HER MAJESTY'S STATIONERY OFFICE

To be purchased from
York House, Kingsway, London W.C.2
423 Oxford Street, London W.1
13A Castle Street, Edinburgh 2
109 St. Mary Street, Cardiff
39 King Street, Manchester 2
50 Fairfax Street, Bristol 1
2 Edmund Street, Birmingham 3
80 Chichester Street, Belfast 1
or through any bookseller

Printed in England

R. & M. No. 3148

S.O. Code No. 23-3148